ISSN 0503-1540

La mer

Tome 39 Numéro 2 Mai 2001

La Société franco-japonaise
d'océanographie
Tokyo, Japon

Note pour la présentation des manuscrits

La mer, organe de la Sociét franco-japonaise d'océanographie, publie des articles et notes originaux, des articles de synthèse, des analyses d'ouvrages et des informations intéressant les membres de la société. Les sujets traités doivent avoir un rapport direct avec l'océanographie générale, ainsi qu'avec les sciences halieutiques.

Les manuscrits doivent être présentés avec un double, et dactylographiés, en *double interligne*, et au recto exclusivement, sur du papier blanc de format A4 (21×29.7 cm). Les tableaux et les légendes des figures seront regroupés respectivement sur des feuilles séparées à la fin du manuscrit.

Le manuscrit devra être présenté sous la forme suivante:

1° Il sera écrit en japonais, français ou anglais. Dans le cadre des articles originaux, il comprendra toujours le résumé en anglais ou français de *200 mots* environs. Pour les textes en langues européennes. il faudra joindre en plus le résumé en japonais de *500 letters* environs. Si le manuscrit est envoyé par un non-japonophone, le comité sera responsable de la rédaction de ce résumé.

2° La présentation des articles devra être la méme que dans les numéros récents; le nom de l'auteur précédé du prénom *en entier*, en minuscules; les symboles et abréviations standards autorisés par le cometé; les citations bibliographiques seront faites selon le mode de publication: article dans une revue, partie d'un livre, livre entier, etc.

3° Les figures ou dessins originaux devront être parfaitement nettes en vue de la réduction nécessaire. La réduction sera faite dans le format 14.5×20.0 cm.

La premiére épreuve seule sera envoyée à L'auteur pour la correction.

Les membres de la Société peuvent publier 7 pages imprimées sans frais d'impression dans la mesure à leur manuscrit qui ne demande pas de frais d'impression excessift (pour des photos couleurs, par exemple). Dans les autres cas, y compris la présentation d'un non-membre, tous les frais seront à la charge de l'auteur.

Cinquante tirés-à-part peuvent être fournis par article aux auteurs à titre gratuit. On peut en fournir aussi un plus grand nombre sur demande, par 50 exemplaires.

Les manuscrits devront être adressés directement au directeur de publication de la Société: Y. YAMAGUCHI, Université des Péches de Tokyo, Konan 4-5-7, Minato-ku, Tokyo, 108 Japon; ou bien au rédacteur étranger le plus proche: H. J. CECCALDI, EPHE, Station marine d'Endoume, rue Batterie-des-Lions, 13007 Marseille, France; E. D. GOLDBERG, Scripps Institution of Oceanography, La Jolla, California 92093, Etats-Unis; ou T. R. PARSONS, Institute of Ocean Sciences, P.O.Box 6000, 986OW, Saanich Rd., Sidney, B. C., V8L 4B2, Canada.

La mer 39 : 63-75, 2001
Société franco-japonaise d'océanographie, Tokyo

Numerical modeling of density-driven current in Tokyo Bay

Ivonne M. RADJAWANE*, Masaji MATSUYAMA*, Yujiro KITADE* and Toru SUZUKI**

Abstract : Density-driven current induced by fresh water discharge from rivers in Tokyo Bay was numerically investigated by multi-level model. The experiment was focused on the density distribution and motion in the inner bay under the summer stratification by giving the monthly mean discharge. The low density water from the river mouth spreads asymmetrically in the surface layer of the basin by influence of Coriolis' force and moves along the coast on its right hand side with maximum velocity of 3-5 cm s^{-1}. In the surface layer, the low density water forms a coastal-trapped plume. The flow toward the river mouth is formed just beneath the surface layer, and is very weak in comparison with the surface outward flow. The inflows may be induced by the outward flow at the surface as the entrainment.

Key words : *Tokyo Bay, three-dimensional model, density-driven current, river discharge, salinity distribution, Coriolis effect, anticyclonic circulation*

Introduction

Tokyo Bay is located at the central part of the main island of Japan, facing to the Pacific Ocean (Fig. 1). The bay is separated in two parts, i.e., the inner and outer bays. The mean depth, bay length and width of the inner bay are 18 m, 80 km and 20-30 km, respectively.

The surface circulation consists of wind-driven, density-driven and tide-induced residual currents (UNOKI, 1993). The tide-induced residual current is not significant except the eastern area near the connection between the inner and outer bays. This is already clarified by the observation (UNOKI *et al.*, 1980) and numerical modeling (e.g., IKEDA *et al.*, 1981; GUO and YANAGI, 1994). The existence of wind-driven current was indicated by the moored current measurements(Hasunuma, 1979; UNOKI, 1985). SUZUKI and MATSUYAMA (2000) indicated that the main results of the observation at moored stations are simulated as the wind-driven current by using a three-dimensional model. They showed the importance of baroclinic response to the wind in the northern region of the stratified Tokyo Bay. On the other hand, FUJIWARA *et al.* (1997) showed that the anticyclonic circulation in the upper layer is formed near bay head of rectangular bay by freshwater discharge, and they suggested the importance of density-driven current in the surface circulation near the bay head. They explained an anticyclonic circulation in the upper layer to be caused by horizontal divergence associated with upward entrainment, which is a part of the estuarine circulation and means the importance of stratification by earth's rotation. We wonder how mechanism of the strong upward entrainment is induced by the weak discharged flow. Their study didn't sufficiently evaluate contribution of density-driven current due to river discharge to residual current. Therefore, the study of density-driven current induced by the river discharge in Tokyo Bay is required to understand the residual current, which advects various properties from the bay to the open sea.

In the present study, we try to investigate the density current induced by the discharged water from the rivers in Tokyo Bay, using the three-dimensional numerical model. We focus on the behavior and structure of low density water around the estuary.

* Laboratory of Physical Oceanography, Dept. of Ocean Sciences, Tokyo University of Fisheries, 4-5-7 Konan, Minato-Ku, Tokyo 108-8477, Japan
** Marine Information Research Center, Japan Hydrographic Association, Mishima Building 5F, 7-15-4, Ginza, Chuo-Ku, Tokyo 104-0061, Japan

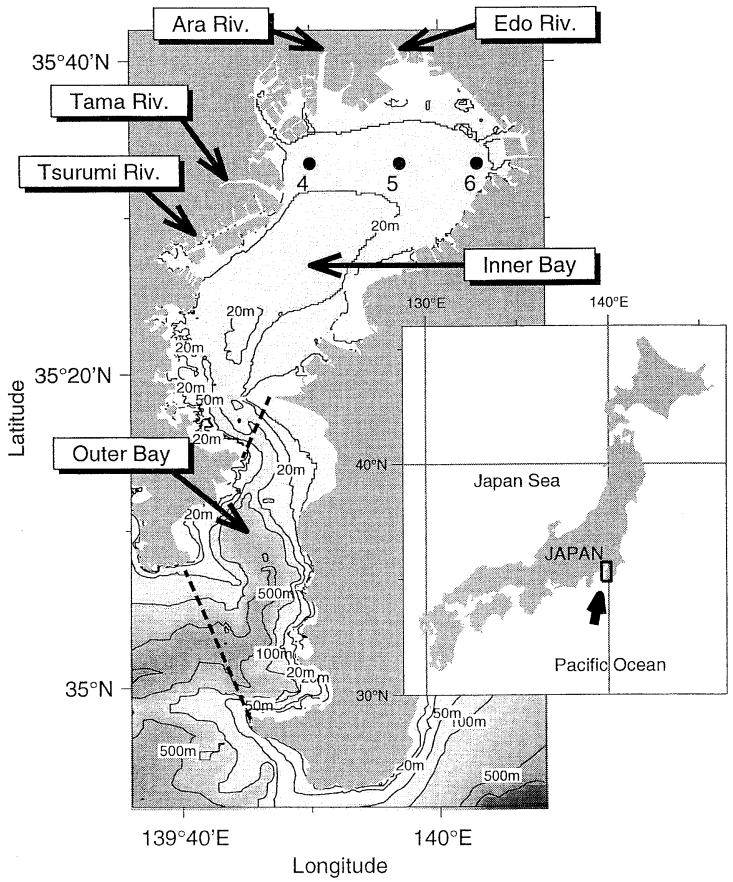

Fig. 1. Bottom topography of Tokyo Bay and location of the observation sites in Tokyo Bay. Numerals on bottom contours are in meters. Station K is the CTD station of Kanagawa Prefectural Fisheries Research Institute. The filled circles with station numbers indicate the CTD stations of the 3rd Regional Coast Guard Headquarters, Japan Coast Guard.

River discharge in Tokyo Bay

The data of river discharge are mostly observed at the mouth of each river. We need the data of river discharge for the boundary condition of the numerical modeling as forcing. The discharge data at main four rivers, i.e., Edo, Ara, Tama and Tsurumi Rivers, are used for experiments. In this study, we focus on the low salinity water at the sea surface along the western coast of Tokyo Bay in August. Figure 2 shows the daily-mean discharge volume of each river and total discharge volume during the period from August 1 to 31, 1995, from the "Report of River Discharge Data 1995". The largest discharge volume was Edo River, and the smallest was Tsurumi River. The monthly mean of total volume discharged into Tokyo Bay was 110 m^3s^{-1}, and it ranged from 75 m^3s^{-1} to 250 m^3s^{-1} in this period. Based on Annual Report on River Discharge data in Japan in 1979, GUO and YANAGI (1998) used the total freshwater volume of 130 m^3s^{-1}, i.e., Edo River, Ara River, Tama River and Tsurumi River are 70, 30, 20 and 10 m^3s^{-1}, respectively.

Model description

We consider a stratified, rotating, incompressible fluid, and use a rectangular coordinate system on an f-plane. Figure 3 shows the model configuration of Tokyo Bay. The $x,y,$ and z-axes are taken in southeastward, northeastward and vertically upward from the mean

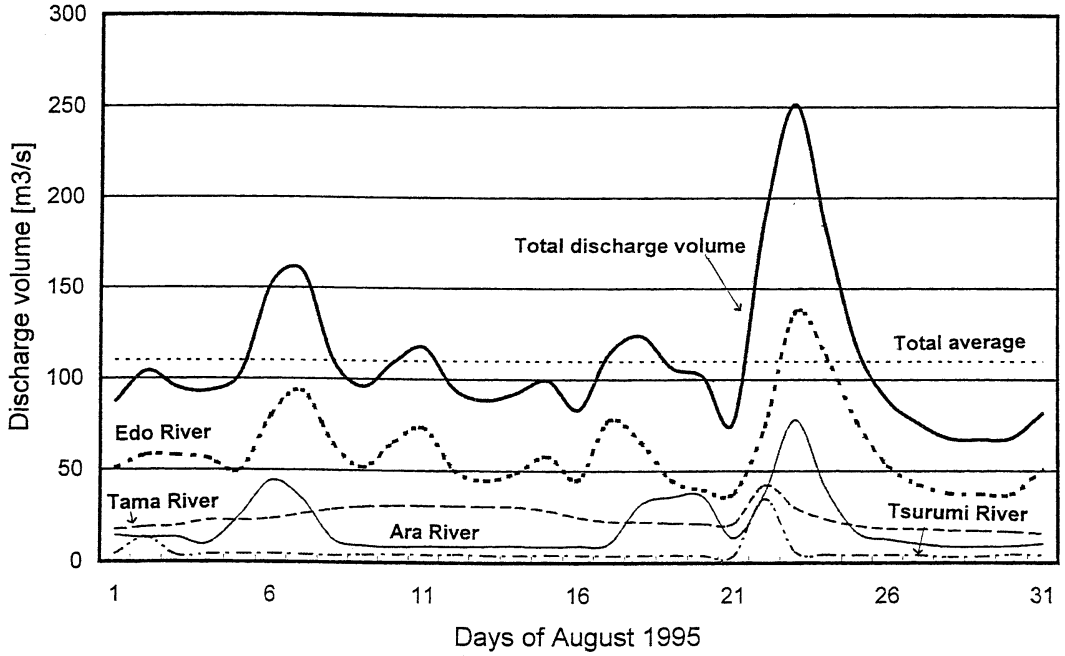

Fig. 2. Daily-mean river discharged volume of main rivers in Tokyo Bay during August 1995.

sea-surface level, respectively. The basic equations are as follows;

$$\vec{u}_t+\vec{u}\cdot\nabla\vec{u}+w\vec{u}_z+f\vec{k}\times\vec{u}=-\frac{1}{\rho_0}\nabla\rho+A_h\nabla^2\vec{u}+A_v\vec{u}_{zz}$$

$$\rho g=-p_z$$

$$\nabla\cdot\vec{u}+w_z=0$$

$$\rho_t+\vec{u}\cdot\nabla\rho+w\rho_z=K_h\nabla^2\rho+\frac{K_v}{\delta}\rho_{zz}$$

where $\vec{u}$ is the horizontal velocity vector (u,v), w the vertical velocity, ∇ the horizontal gradient operator, ∇^2 the Laplacian operator, f the Coriolis' parameter, $\vec{k}$ unit vector of vertical axis, ρ_0 the reference density, ρ the density, p the pressure and g the gravitational acceleration. A_h, A_v, K_h, and K_v are the coefficients of the horizontal and vertical eddy viscosity and the coefficients of the horizontal and vertical diffusivity, respectively. The symbol δ is the instantaneous convective adjustment parameter and is used to maintain a stable stratification in the model (SUGINOHARA, 1982). It is defined as follows:

$$\delta=\begin{cases}1 & for \quad \dfrac{\partial\rho}{\partial z}\le 0\\[2ex] 0 & for \quad \dfrac{\partial\rho}{\partial z}>0\end{cases}$$

A non-slip and no normal density flux conditions are adopted at the coastal boundary as follows:

$$\vec{u}=0,$$

$$\frac{\partial\rho}{\partial n}=0,$$

where n denotes the normal component to the coast. The bottom boundary conditions are adopted as follows:

$$\frac{\partial\rho}{\partial z}=0,$$

$$A_v\left(\frac{\partial u}{\partial z},\ \frac{\partial v}{\partial z}\right)=C_bU_B(u_B,\ v_B)$$

where $U_B=\sqrt{u_B^2+v_B^2}$ is the current speed, with u_B and v_B the velocity components just above the sea bottom in the x and y directions, respectively, and C_b is the coefficient of bottom friction. At the sea surface $(z=\eta)$, no wind stress is given.

An Orlanski Radiation Condition (ORLANSKI,

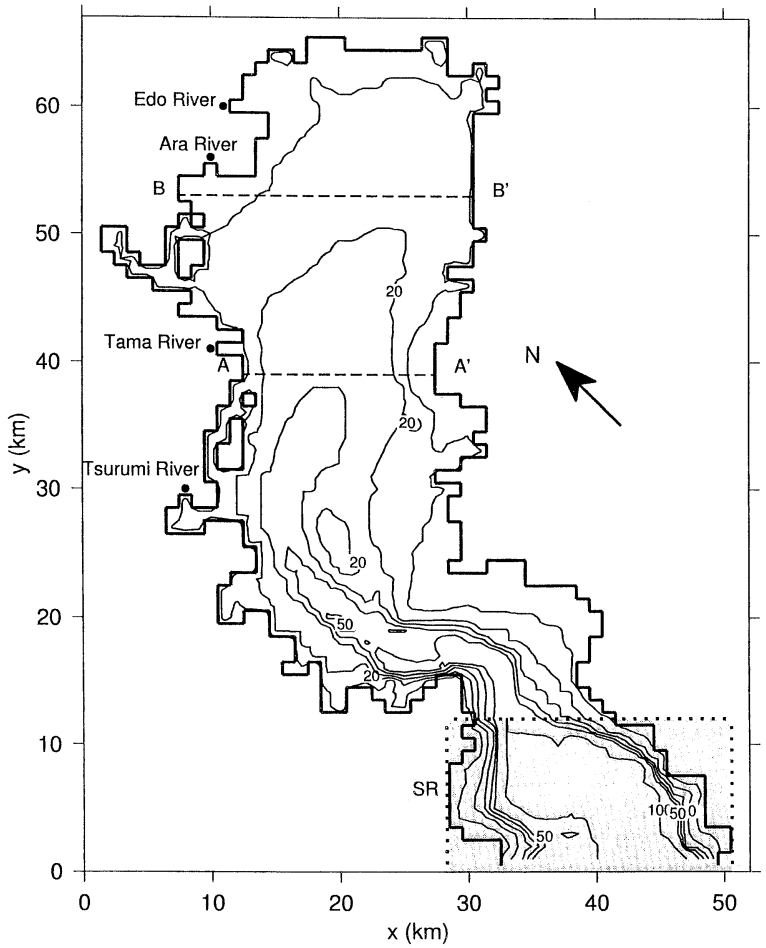

Fig. 3. Schematic view of the model. Numerals on bottom contours are in meters. The sponge region (SR) is imposed at $0<y<12$km and the area is drawn by the dotted lines. The filled circle indicates the mouth of the main river. Dashed lines (A–A' and B–B') are used for model cross sections.

1976) is imposed to velocity components, u, v and elevation of sea surface η at the bay mouth, i.e., the southern boundary at $y=0$.

$$\frac{\partial \phi}{\partial t} \pm c \frac{\partial \phi}{\partial y} = 0$$

where

$$c = \begin{cases} \dfrac{\Delta y}{\Delta t} & if \quad \mp \dfrac{\partial \phi}{\partial t} \Big/ \dfrac{\partial \phi}{\partial y} \geq \dfrac{\Delta y}{\Delta t} \\ \mp \dfrac{\partial \phi}{\partial t} \Big/ \dfrac{\partial \phi}{\partial y} & if \quad 0 < \mp \dfrac{\partial \phi}{\partial t} \Big/ \dfrac{\partial \phi}{\partial y} \geq \dfrac{\Delta y}{\Delta t} \\ 0 & if \quad \mp \dfrac{\partial \phi}{\partial t} \Big/ \dfrac{\partial \phi}{\partial y} \leq 0 \end{cases}$$

where Δt and Δy are a time step and grid size of y-direction, respectively. Moreover the sponge region of 12 km length from the bay mouth is added. Within this region the bottom friction coefficient is exponentially increased from its interior value to four times that value at the open boundary (RØED and COOPER, 1987).

The basic density stratification is given in Fig. 4 as a representative one in summer. The data were obtained at Stn. K (Fig. 1) by Kanagawa Prefectural Fisheries Research Institute on August 6, 1979. The observed density stratification from the sea surface to 30m depth is used in this model. The density beneath 31m depth is assumed as uniform, and it is the same value as that at 30m depth. Density of

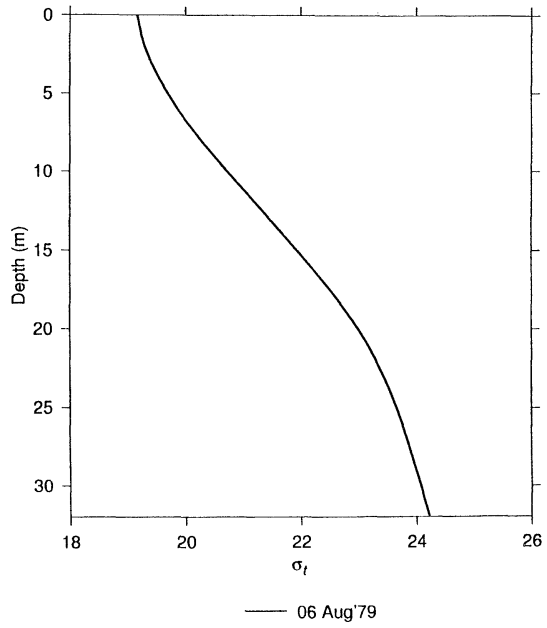

Fig. 4. Basic density (σ_t) stratification at the hydro-cast station observed by Kanagawa Prefectural Fisheries Research Institute on August 16, 1979.

Table 1. Discharge volume (m^3s^{-1}) of each river used in the model.

Riber Name	Case 1 (typical case)	Case 2 (flood case)
Edo River	70	200
Ara River	30	70
Tama River	20	40
Tsurumi River	10	15
Total	130	325

freshwater at each river mouth is assumed as 1.0100 g cm^{-3}, while the ambient density at the sea surface is 1.0192 g cm^{-3}. Two cases of the numerical experiments were performed;(1) Case 1 is the typical volume of discharge water in summer, and (2) Case 2 is the flood case (Table 1). Water in the whole bay is at rest initially. To avoid the initial shock waves, the river velocity is gradually increased in two hours from zero to the given value. The horizontal grid size is 1km and vertical grid is 1m from the sea surface to 31m depth. The bottom layer is taken from 31m to the sea bottom in the model. Time step is 10 seconds. To get well-established plume shape, the model is running for 12 days. For computational efficiency, the maximum water depth is limited by 100m depth.

The following values are used for numerical computations; $f=8.44\times10^{-5}$ s^{-1} (at 35.5° N), g = 980 cm s^{-2} and $\rho_0 = 1.0000$g cm^{-3}. The following coefficients for the calculation are based on the previous numerical studies (SUGINOHARA 1982; SUZUKI and MATSUYAMA, 2000); $A_h = 1.0\times10^6 cm^2 s^{-1}$, $A_v = 1.0 cm^2 s^{-1}$, $K_h = 1.0\times10^5$ cm^2 s^{-1}, $K_v = 1.0$ cm^2 s^{-1} and $C_b = 2.6\times10^{-3}$. The basic equations are numerically solved by a semi-implicit finite-difference method using a non-staggered Arakawa-C grid.

Results

Figure 5 shows the distributions of horizontal current vector and density at 0.5m depth from 0.5 day to 12days after the initial state. At

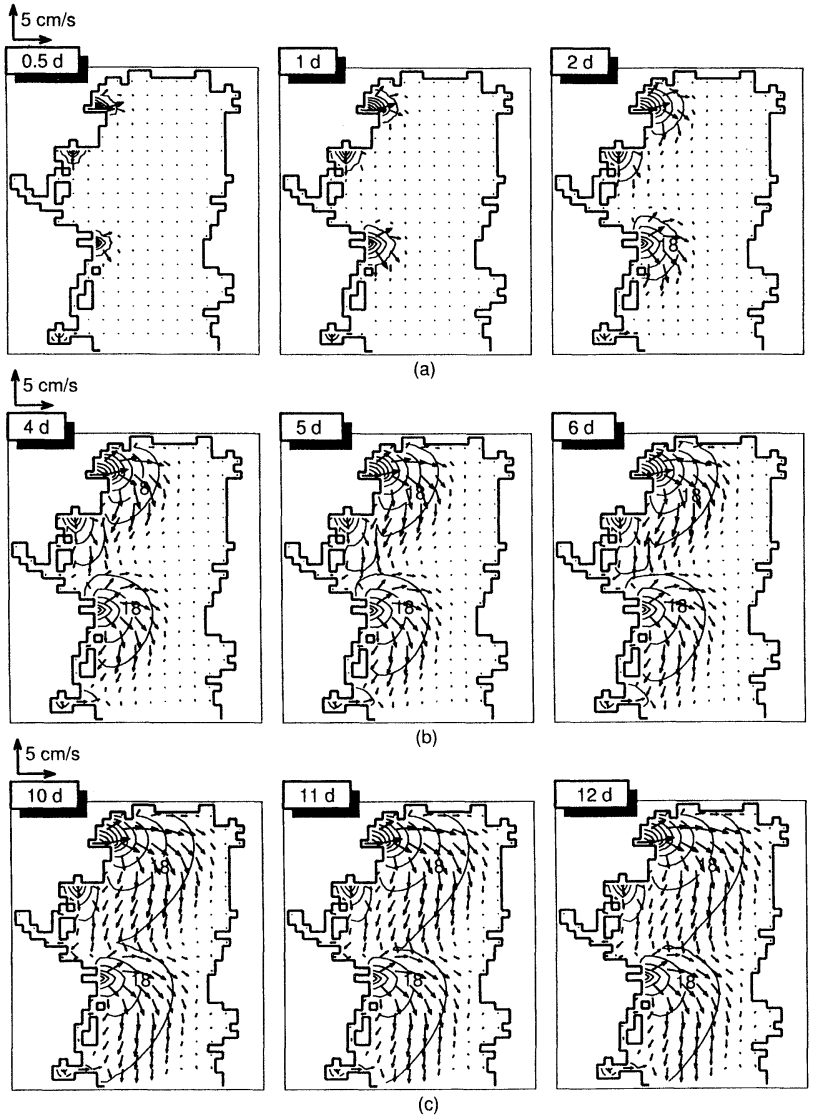

Fig. 5. Evolution of density and velocity distributions at 0.5 m depth after 0.5, 1, and 2 days (upper panel), after 4, 5 and 6 days (middle panel), and after 10, 11 and 12 days (lower panel) from initial stage for Case 1 (typical case). Isopycnal interval is σ_t of 1.0.

0.5 and 1day, low density water can be found in the limited region near the mouth of the Edo, Ara and Tama rivers. At 2 days, the low density region is clearly formed near the mouth of the rivers, and the contour lines mostly form the semicircle plume. The low density region slightly extends toward the bay mouth. At 4, 5 and 6 days, the low density region still grows in horizontal and slightly extends along the western coast. The current vector has a right angle with the density contours near the river mouth, while it diagonally crosses the contours in the offshore region. Maximum velocity is 3 −5 cm s^{-1} and it is not so large. These current patterns show almost steady state at 6 days except near boundary between the low density water and bay water, but the density contour lines slowly extend toward the east and south

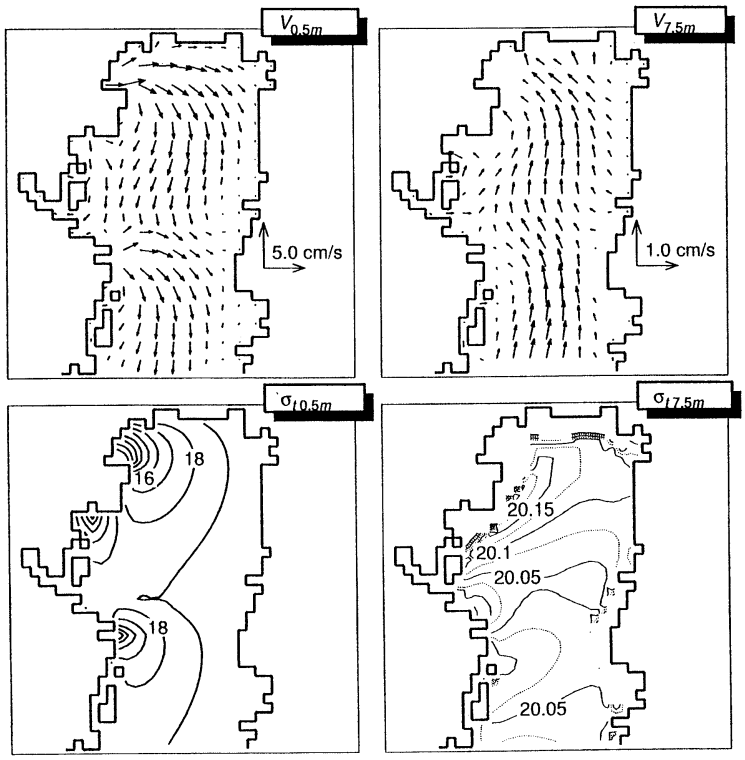

Fig. 6. Horizontal distribution current and density at 0.5m (upper) and 7.5m (middle) depths after 12 days. Isopycnal interval is as follows: st of 1.0 for st<19.00 and st of 0.025 for σ_t>19.00.

even at 12 days. The low density water moves toward the bay mouth along the western coast. The large cells are formed near the river mouth and both cells have nature of the clockwise circulation. The high pressure, i.e., high sea level region is formed by the river discharge as indicated by the hydraulic model experiments (MICHIDA, 1983; KITAMURA and NAGATA, 1983).

Figure 6 shows the horizontal distributions of velocity and density at two depths for the inner bay at 12 days. Two depths of 0.5m and 7.5m are selected as the representative of the surface and middle layers, respectively, to describe the current and density patterns. In the surface layer, the current direction is southward along the western coast following the geometric shape of the bay. Maximum velocity is found nearby the river mouth in the western part of the bay. The low density water flows out in the surface layer near the river mouths, and low density region is formed along the western coast. In the middle layer, the current vector direction is toward the bay head beneath the outward flow. This inward current may be induced by the outward flow in the surface layer. But this inward current is very weak in comparison with the surface outward one. The density in the middle layer is slightly higher near the mouth of the rivers than other region, suggesting existence of upwelling associated with entrainment.

Figure 7 shows the vertical sections of density, cross-bay and along-bay components of current across the bay at y = 38km (A–A' section shown in Fig. 3) after 12 days from the initial stage. The section is selected as the representative one to observe the density current affected by the Edo River, Ara River and Tama River. The density contour lines above 5m depth rise up from the west to the east in the bay. Below this depth, the contour lines are almost in horizontal. The contour lines of σ_t = 19 and below this value outcrop at the sea surface in the region between the west coast and

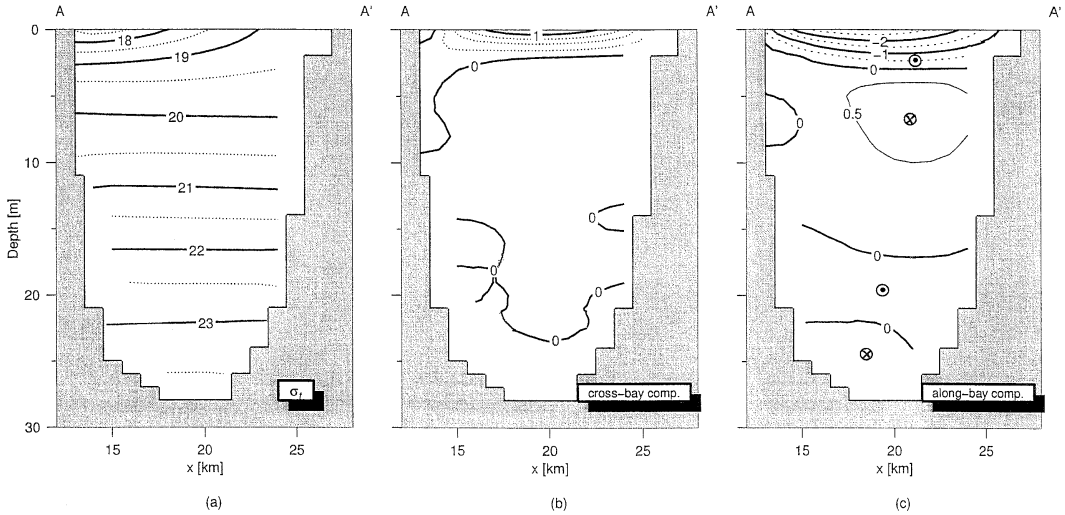

Fig. 7. Cross sections along A–A' line (y =40 km) for σ_t(a), cross-bay current (b) and along-bay current (c) after 12 days. Contour intervals are σ_t of 0.5 for density distribution, 0.25 cm s^{-1} for cross-bay current and 0.5 cm s^{-1} for along-bay current. Negative and positive velocity indicates outflow and inflow direction, respectively.

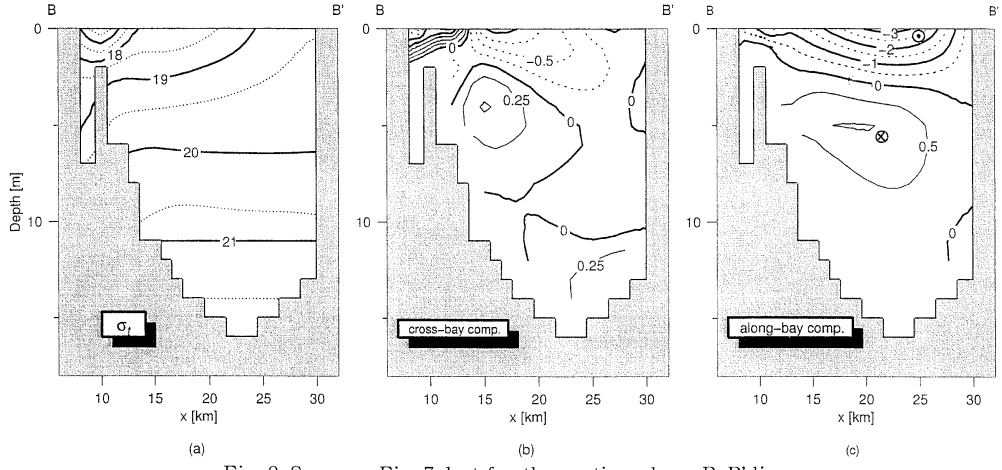

Fig. 8. Same as Fig. 7, but for the section along B–B' line.

center in the bay, that is, the weak density front is formed at the edge of the plume. The horizontal scale of the plume is 5–10 km, longer than the internal radius of deformation of 2–4 km (SUZUKI and MATSUYAMA, 2000). In the surface layer with about 3m thickness, the current is directed to the bay mouth. The strong current is found inside the plume.

Figure 8 shows the cross section at y = 53 km (Section B–B' shown in Fig. 3), which is located 2 km from Ara River at the bay head. The contour lines of the low density water cover wide region at the sea surface. The lines of lower density than σ_t=18.0 concentrate in the narrow region of the west coast. The region of eastward flows in the surface layer mostly agrees with that of the lower density water. The core of southward flow toward the bay mouth exists center of the bay off the low density water and the southward current takes together with weak westward component. This southward or south-southwestward current near the central region is induced by the discharge from Edo River. The frontal structure is

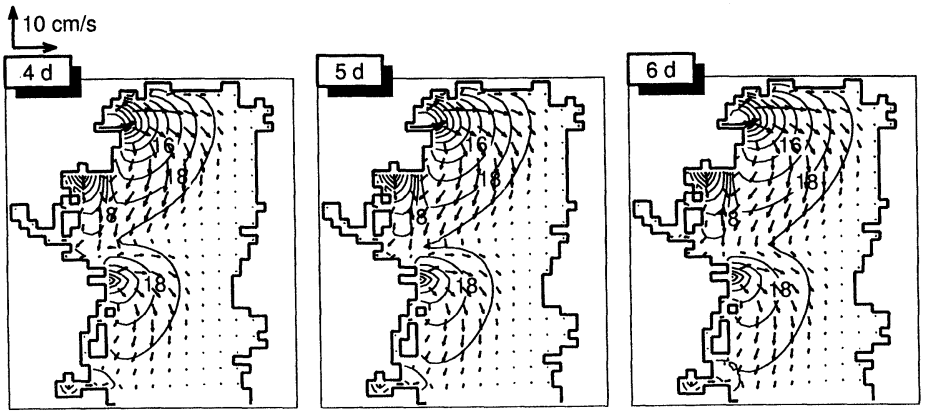

Fig. 9. Density and current distributions near the sea surface after 4, 5 and 6 days for Case 2 (flood case). Isopycnal interval is σ_t of 1.0.

clearly formed near the mouth of Ara River.

Figure 9 shows the current and density distributions at 4, 5 and 6 days for Case 2 (flood case). The low density water spreads faster and occupies wider region in comparison with that for Case 1 (typical case), but their patterns are not different from each other. Maximum velocity is also found near the mouth of rivers and its value is about 10 cm s^{-1}.

The results of numerical experiments using three-dimensional model are summarized as follows. The low density water formed by the river discharge distributes around and off the river mouth in the surface layer along the western coast of the bay in summer. This water flows toward the bay mouth with speed of 3–5 cm s^{-1} in the upper layer for monthly mean discharge, while the inward flows exist just beneath the very weak outward flows for the compensation. We suppose that the current is not easy to be detected by the current measurements at the moored station because of the weak velocity, but the salinity distribution offers the density current pattern.

Discussion

The density-driven current induced by the river discharge is found along the western coast of Tokyo Bay. The low density region in the surface layer is firstly formed in estuary, i.e., off the mouth of rivers and progresses toward the bay mouth along the western coast (Fig. 5). Such features are similar to the behavior of the discharged high temperature water in the coastal area from the power plant (MATSUNO and NAGATA, 1987). The pressure gradient balances to the Coriolis force in the offshore direction, so the low density water progresses along the coast on the right hand side in northern hemisphere for conservation of potential vorticity (e.g., GRIFFITHS, 1986). Figure 10 shows the vertical section of the salinity distribution near the bay head on August 7, 1995, observed by the 3rd Regional Coast Guard Headquarters, Japan Coast Guard. The location of the observation is shown in Fig. 1. The observation line is not taken cross the bay, but is diagonal to the bay axis, i.e., along the latitude line. Although it was the coarse interval from station to station for the observation, the numerical model results (Fig. 8) is similar to the observational ones except for small salinity variation in the eastern side.

Figure 11 shows the salinity distribution at 1m depth in August 7 to 8, 1995, observed by the 3rd Regional Coast Guard Headquarters, Japan Coast Guard, as well. The temperature distribution at the sea surface is not so large difference in the inner bay in summer. The salinity distribution agrees with the density one in the surface layer. The low salinity is found near the mouth of main three rivers along the western side of the bay. The observational result closely resembles the numerical one except near the mouth of Ara River (Fig. 5 and Fig. 9). In Fig. 11, the lowest salinity region is

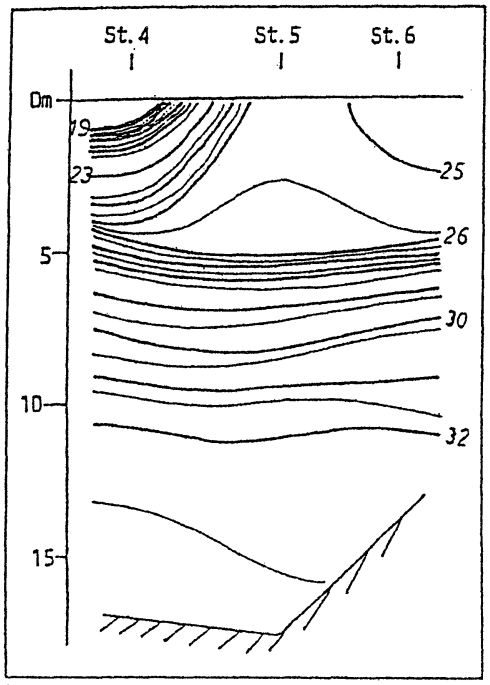

Fig. 10. Vertical distribution of salinity along latitude line at station number 4, 5 and 6 (see Fig. 1) in Tokyo Bay on August 7 to 8, 1995 (after the 3rd Regional Coast Guard Headquarters, Japan Coast Guard).

found off the mouth of Ara River, but not off the mouth of Edo River (Fig. 5). As shown in Fig. 2, Edo River is the largest discharge of the fresh water among the four main rivers, so that the numerical experiments (Fig. 5) shows the low density distributions off the mouth of Edo River. What is reason of the different distributions between observational and numerical results? The observational results are not only affected by the river discharge but also by wind and tide, while the numerical results are affected only by the river discharge. SUZUKI and MATSUYAMA (2000) indicated the important role of the wind-driven current in the inner bay of Tokyo Bay in summer. So, we investigate the wind data at Chiba in August 1995 because tide-induced residual current is not so significant near the bay head. Figure 12 shows the time series of wind vector at Chiba (AMeDAS). The westward wind blows from the morning of August 4 to the afternoon of August 6 and wind direction changes toward southeast after this period. Except about 6 hours in early morning of August 7, the southeastward wind continues during 4–5 days. This wind blows the parallel to the bay head coast, so it is possible to generate an outward Ekman transport. The surface water near the bay head may be moved toward the offshore. This surface water movement may give the explanation for the disappearance of the low salinity water off the mouth of Edo River in the observation.

The numerical experiments also supply a significant feature in the density-driven current induced by the river discharge into Tokyo Bay. It is an upwelling generated by the entrainment of the lower layer water due to the surface outflow. As expected, the inward flow of the lower layer is very weak. The anticyclonic circulation around the river mouth is closely related to the high-pressure region at the sea surface generated by the outflow from rivers. The anticyclonic circulation induces the upwelling in the middle layer. The high density water was found in the middle layer near the river mouth, suggesting the upwelling associated with the entrainment (Fig. 6). The

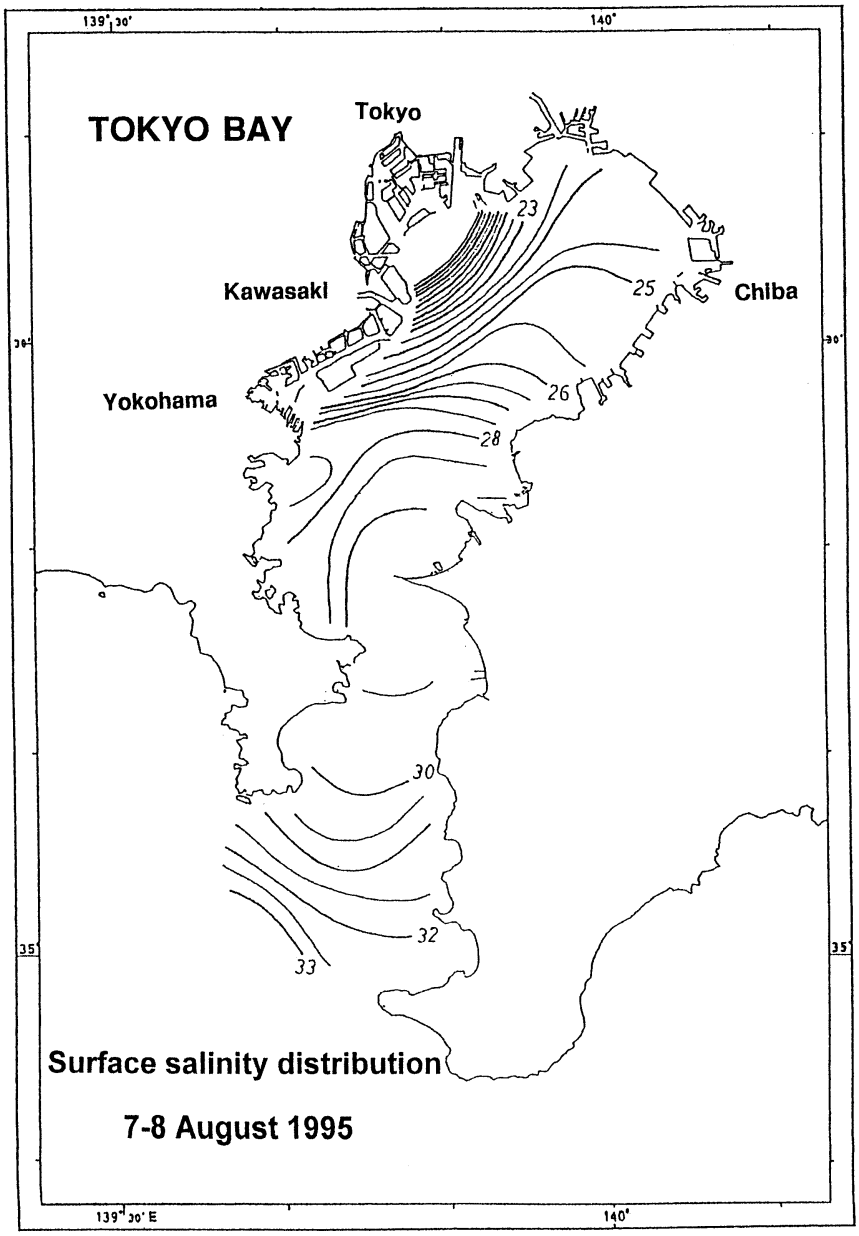

Fig. 11. Horizontal distribution of salinity at 1m depth on August 7 to 8, 1995 in Tokyo Bay (after the 3rd Regional Coast Guard Headquarters, Japan Coast Guard).

detailed discussion will be required to clarify the local upwelling near the mouth by using a simple model.

Summary

The density-driven current is examined as the behavior and structure of the low density water discharged from the rivers, using the three-dimensional numerical model. The low density water spreads in the surface layer from river mouth to the inner bay and makes the anticyclonic circulation after 2–4 days from the

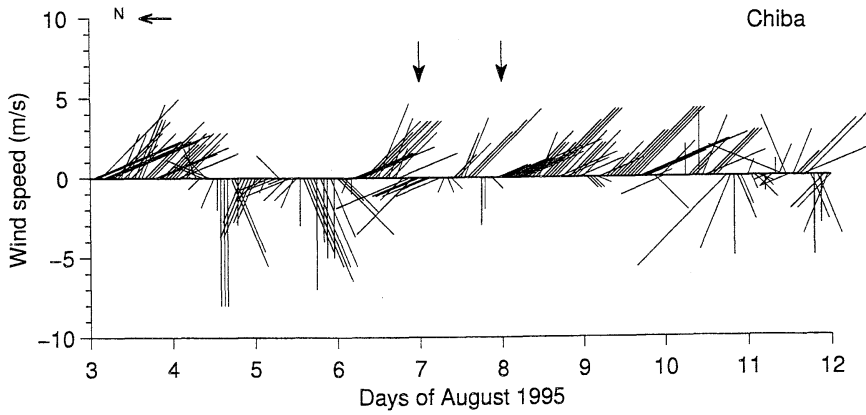

Fig. 12. Time series of wind vectors at Chiba AMeDAS Station during August 3–12, 1995. Two thick arrows indicate the observation time of data sampling of salinity and temperature as shown in Fig. 10 and Fig. 11.

initial state for the mean volume of river discharge. After this time, the water moves toward the bay mouth along the western coast with maximum velocity of 3–5 cm s^{-1}. The flow toward the river mouth is formed just beneath the surface layer, and is very weak in comparison with the surface outward flow. The inflows may be induced by the outward flow at the surface as the entrainment.

The density distribution calculated from the numerical experiments almost resembles the observed salinity distribution at the surface layer along the western coast of the bay except near the mouth of Ara River. Therefore the three-dimensional model is suitable to clarify salinity and temperature distribution in detail for fresh water injection from rivers and power plant. GUO and YANAGI (1998) and TANAKA *et al.* (1998) studied the residual current in the stratified Tokyo Bay by the three-dimensional model. Both papers included all factors such as wind, tide and river discharge in the model, so that the numerical model did not effectively extract the characteristics of density-driven current. The detailed numerical study is required to comprehend an individual phenomenon, i.e., wind-driven current, density-driven current and tidal current.

Acknowledgements

We would like to thank Dr. J. YOSHIDA and members of Physical Oceanography Laboratory, Tokyo University of Fisheries for their fruitful discussion on this study. We appreciate various comments of anonymous referees which improved the original manuscript. The numerical experiments were performed in Data Processing Center at Tokyo University of Fisheries. The observational data were offered from the 3rd Regional Coast Guard Headquarters, Japan Coast Guard. AMeDAS data were offered from Japan Meteorological Agency. This study is partly supported by Grand-in-Aid for Scientific Research 10640420 from the Japan Ministry of Education, Science and Culture.

References

FUJIWARA T., L.P. SANFORD, K. NAKATSUJI and Y. SUGIYAMA (1997): Anti-cyclonic circulation driven by the estuarine circulation in a gulf type ROFI. J. Marine Sys., **12**, 83–99.

GRIFFITHS, R. W. (1986): Gravity currents in rotating systems. Ann. Rev. Fluid Mech., **18**, 59–89.

GUO, X. and T. YANAGI (1994): Three dimensional structure of tidal currents in Tokyo Bay, Japan. La mer, **32**, 173–185.

GUO, X. and T. YANAGI (1998): Variation of residual current in Tokyo Bay due to increase of fresh water discharge. Cont. Shelf Res., **18**, 677–693.

HASUNUMA, K. (1979): The specific currents in Tokyo Bay. Bul. Coast. Oceanogr. Japan, **16**, 27–75 (in Japanese).

IKEDA, K., M. MATSUYAMA and M. TSUJI (1981): Effect of the wind on the current in Tokyo Bay. Umi to Sora, **57**, 31–40 (in Japanese with English abstract and captions).

KITAMURA, Y., and Y. NAGATA (1983): Behavior of fresh water injected at the surface of a uniformly rotating ocean. J. Oceanogr. Soc. Japan, **39**, 94–105.

MATSUNO, T. and Y. NAGATA (1987), Numerical study of the behavior of heated water discharged into the ocean; part I: the effect of earth's rotation. J. Oceanogr. Soc. Japan, **43**, 295 –308

MICHIDA, Y.(1983): Behavior of low density water in a uniformly rotating ocean. Master Thesis of Science, University of Tokyo. 56pp. (in Japanese).

ORLANSKI, I. (1976): A simple boundary condition for unbounded hyperbolic flows. J. Comput. Phys., **21**, 251–269.

RØED L.P. and C. K. COOPER (1987): A study of various open boundary conditions for wind- forced barotropic numerical ocean models. *In*: Three-Dimensional Models of Marine and Estuarine Dynamics, Elsevier Oceanography Series, NIHOUL, J. C. J., and B.M. JAMART. (eds.) **45**, Netherlands, Elsevier Publishers B.V., 305–335.

SUGINOHARA, N. (1982): Coastal upwelling: Onshore-offshore circulation, equatorward coastal jet and poleward undercurrent over a continental shelf-slope. J. Phys. Oceanogr., **12**, 272–284.

SUZUKI, T. and M. MATSUYAMA (2000): Numerical Experiments on Wind-induced Circulation in Stratified Tokyo Bay, Japan. Est. Coast. Shelf Sci., **50**, 17–25.

TANAKA, M., S. INAGAKI and G.S. STELLING (1998): Numerical simulation of flow under the stratified condition in Tokyo Bay, Japan. *In*: Hydroinfor matics '98, Babovic and Larsen, (eds.) Balkema, Rotterdam, 1463–1468.

UNOKI, S., M. OKAZAKI and H. NAGASHIMA (1980): The circulation and oceanic condition in Tokyo Bay. Report of Phys. Oceanogr. Lab. Phys.-Chem. Inst., No **4**, 262 pp. (in Japanese).

UNOKI, S. (1985): Tokyo Bay, its physical aspect, *In*: Coastal Oceanography of Japanese Islands, Tokai University Press, Tokyo, 341–361 (in Japanese).

UNOKI, S. (1993): Physical Oceanography of Coastal Area. Tokai University Press, Tokyo, 672 pp, (in Japanese).

Received September 19, 2000
Accepted November 28, 2000

La mer 39 : 77-85, 2001
Société franco-japonaise d'océanographie, Tokyo

Seasonal variation of water characteristics in the northern coastal area of Java

Suhendar I SACHOEMAR* and Tetsuo YANAGI**

Abstract : Seasonal variation of water characteristics in the northern coastal area of Java was investigated to understand the causal factors of its variability and to evaluate the water quality status in the future within this region. Water temperature, salinity and density in the northern coastal area of Java Sea seasonally varied corresponding to the monsoon. Water temperature in January(wet season)was lower than that in September(dry season) as well as for salinity and density. Nutrient concentration was influenced by discharge of the local river and local coastal topography and was also affected by surface current corresponding to the monsoon. Phosphate was high in January at the central part and in September at the western part. Silicate was high in January at the eastern part and in September at the western part as well as for nitrate. Redfield ratio in the whole part of the northern coastal area of Java was lower than 16 and nitrate may act as the limiting factor for the primary production within this region. Chlorophyll-*a* was high in January at the central and western parts of Java due to large supply of nutrients by river discharge. While in the eastern part of Java, high conecentration of chlorophyll-*a* in September was due to the nutrients supply from the eastern region of Indonesia by surface current.

Key words : *seasonal variation, water characteristics, northern coastal area of Java*

1. Introduction

Shince more than 2 decades ago, the northern coastal area of Java has been developed as the most important area for the economical growth in the Java Island. The rapid development of the agriculture activities such as rice field, shrimp culture as well as the industrial and housing estate within this area are suspected to have caused some negative excess on the degradation of the environmental condition (ONGKOSONO *et al*, 1990; ONGKOSONO, 1992; PRASENO, 1995; NURDJANA, 1997). The appreciable pollution and waste deposition from those activities that are carried by river discharges, ultimately cause the water quality deterioration in the coastal sea within this region.

To conserve this area for sustainable utilization in the future and to select the area for suitable activities, an observation of water characteristic along the coastal area of Java is necessary to be established in order to understand the water quality status as a basic knowledge on the regional planning. To achieve such objective, since 1979-1981, the Ministry of the Environmmental Affair, Indonesia has collaborated with The Research Institute for Oceanography-LIPI to collect the numerous data of physical, chemical and biological oceanography as a basic information to develop various kind activities on the basis of water quality status. Since the seasonal change has trong affected on the performance of the agricultural production, e.g. for shrimp culture (SACHOEMAR and YANAGI, 1999), the information of water quality status corresponding to the seasonal variation becomes important to provide a proper management and planning of shrimp culture activity. Currently, however, there is almost no information on the water quality status corresponding to the seasonal variation along the northern coastal area of Java, except partially on the small area with limited data in

* Interdisciplinary Graduate School of Engineering Sciences, Kyushu University, Fukuoka, Japan
** Research Institute for Applied Mechanics, Kyushu University, Fukuoka, Japan

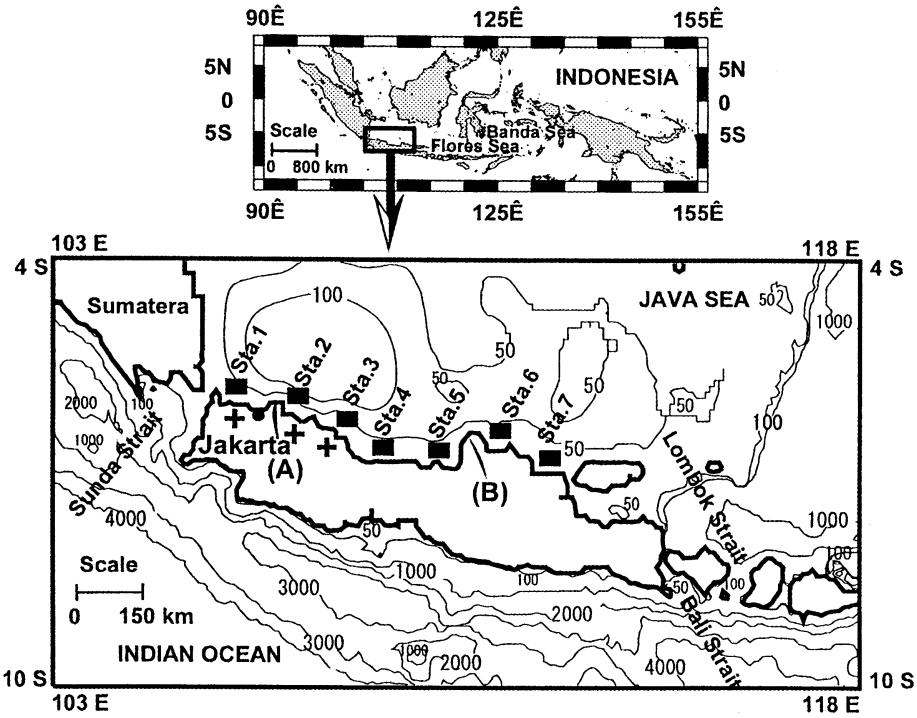

Fig. 1. Maps showing the study area. Bathymetry (meter) and sampling points are inserted. The symbols (A) denotes Citarum river, (B) Serang river and (+) industrial area in the northern coast of Java.

the certain season (ROHILAN, 1992; PRASENO and ADNAN, 1996; PUTRI *et al*, 1999). While a basic knowledge is required to recover the deteriorated water quality due to the excessive pollution during the intense utilization in a long period toward the initial status when the highest production of shrimp was achieved. Hence, the review of water characteristic of the northern coastal area of Java corresponding to the seasonal variation is to be necessary to complete the lack information of the water quality within this region. This information is hoped to be an important information to evaluate the water quality status in the present time for the future sustainable utilization and to understand the causal factors of water quality variability within this region.

2. Data collection and analysis

A series of hpysical, chemical and biological data in January (northwest monsoon) and September (shoutheast monsoon) 1979–1981 were obtained from The Research Institute for Oceanography-LIPI (Lembaga Oceanologi Nashional-LIPI, 1980 and 1981) to study a seasonal variation of water characteristics within this region. Horizontal and vertical data were collected from the study area of 7 regions of western Java (Sta. 1, Sta. 2 and Sta. 3), central Java (Sta. 4 and Sta. 5) and eastern Java (Sta. 6 and Sta. 7) in the northern coastal area of Java (Fig. 1).

Water temperature of the surface, 5m, 10m and 20m depth were measured by thermometer, salinity by Portable Inductive Salinometer model RS-7C. While phosphate, nitrate and silicate were analyzed by spectrophotometric method using Spectronic 20 and 21 of Bausch and Lamb, Germany, with wave length of 885 nm for phosphate, 543 nm for nitrate and 810 nm for silicate (STRICKLAND and PARSON, 1968). Dissolved oxygen was measured by Winkler method (U. S. Navy Hydrographic office, 1959) and chlorophyll-*a* by spectrophotometric

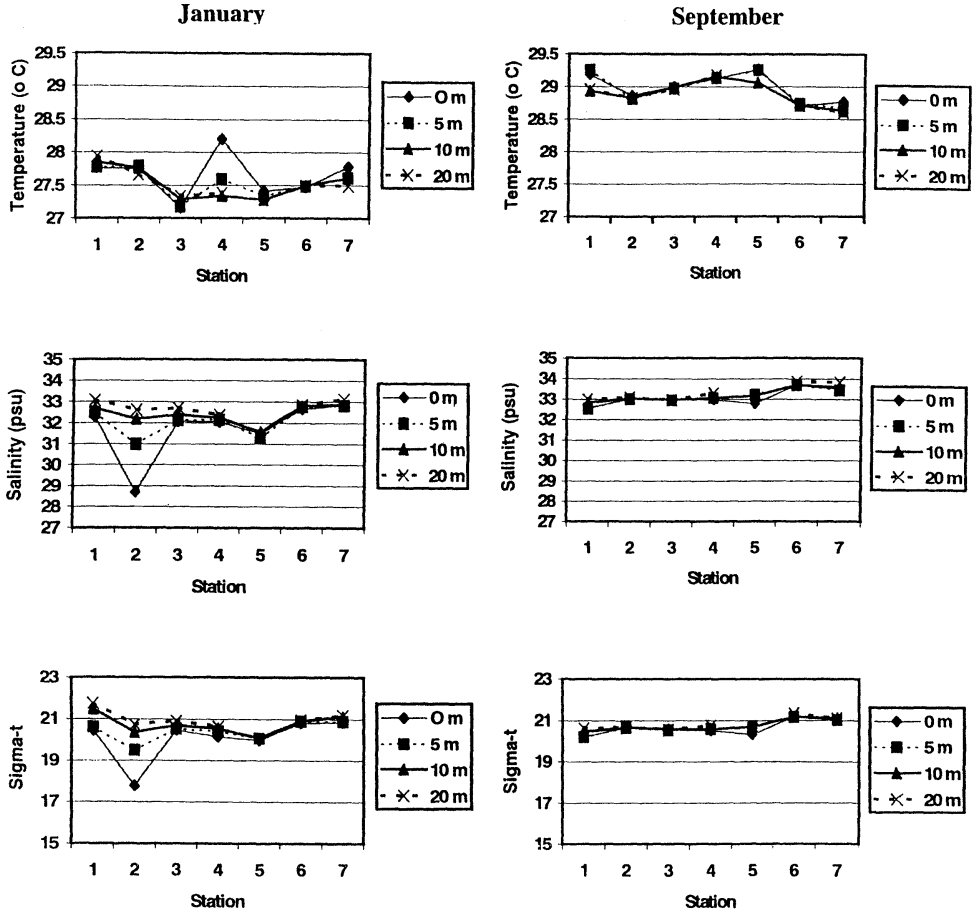

Fig. 2. Horizontal and vertical distributions of water temperature (℃), salinity (psu) and density (sigma-t) in the northern coastal area of Java in January and September 1981.

method using Spectronic 21 model UV-M with wave length of 750, 665, 645 and 630 nm (PARSON and STRICKLAND, 1963). To support this study, air temperature at the observation stations and a series of meteorological data of solar radiation, rainfall, humidity and evaporation at Jakarta derived from 1930–1961 were also collected from Meteorological Agency of Indonesia.

3. Results

Horizontal and vertical distributions of water temperature, salinity and density (sigma-t) in January (northwest monsoon) and September (southeast monsoon) 1981 are shown in Fig. 2. Water temperature in January was lower than that in September. Water temperature in January was within 27.2–28.2℃ with stratified distribution at Sta. 4 of the central part and mixing in the western and eastern parts of Java. In September, water temperature was within 28.6–29.3℃ with vertical mixing in the whole area. Salinity and density in January were relatively lower than those in September, especially for the surface layer of Sta. 2 in the western part of Java. Salinity and density in January were within 28.7–33.1 psu and 17.8–21.7, respectively, with stratified distribution at Sta. 2 of the western part and vertical mixing in the central and eastern parts of Java. In September salinity and density were within 32.6–33.9 psu and 20.2–21.3, respectively, with vertical mixing condition in the whole area.

Horizontal and vertical distributions of

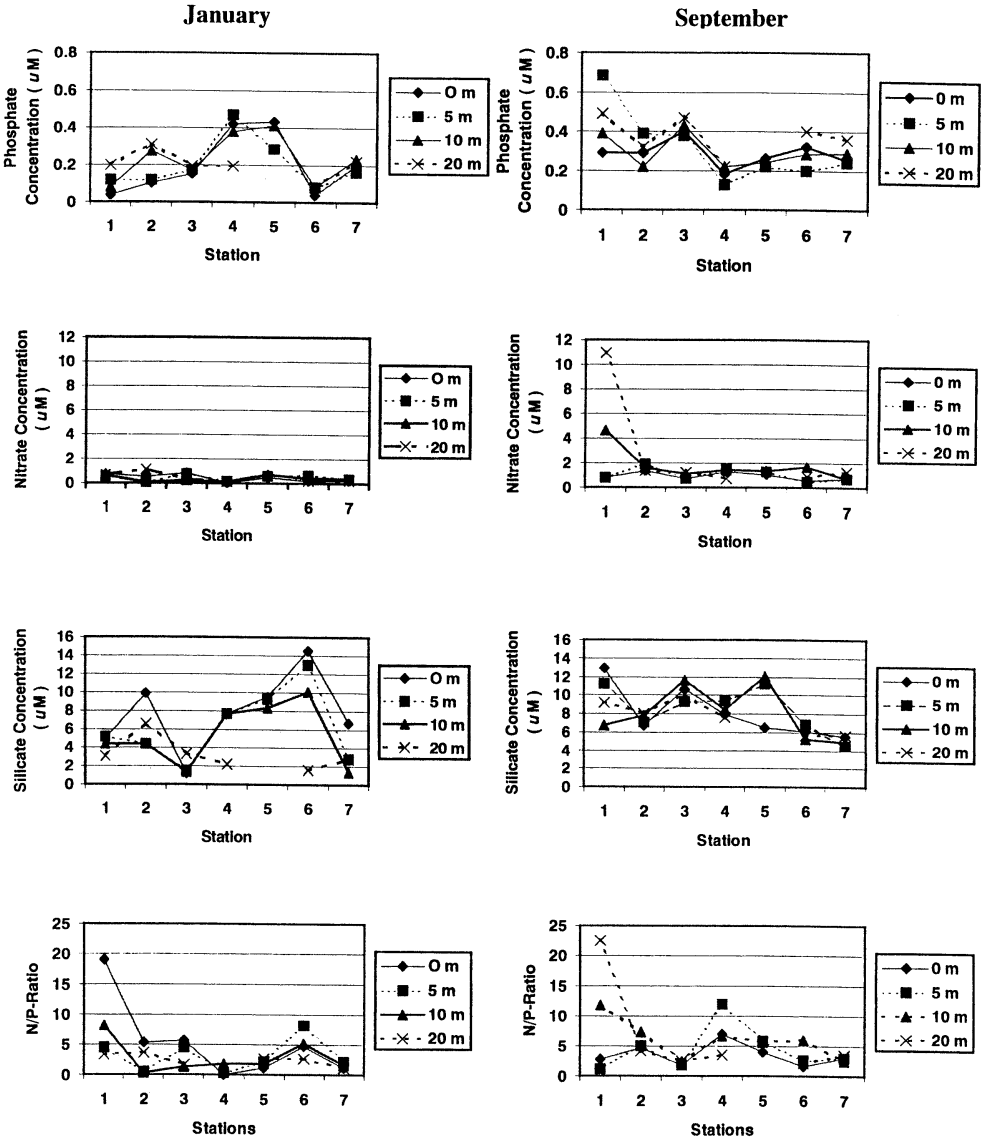

Fig. 3. Horizontal and vertical distributions of phosphate (μM), nitrate (μM), silicate (μM) and N/P-Ratio in the northern coastal area of Java in January and September 1981.

phosphate, nitrate and silicate in January and September 1981 are shown in Fig. 3. Phosphate concentration in January was relatively lower than that in September in the western part and at Sta. 6 of the eastern part. Phoshate concentration in January was within 0.04–0.47 μM and stratified at Stas. 1 and 2 of the western part and at Sta. 4 of the central part. In September, phosphate concentration was within 0.13–0.68 μM and stratified at Sta. 1 of the western part.

Nitrate concentration in January was lower than that in September, especially at Sta. 1 of the western part. Nitrate concentration in January was within 0.14–1.14 μM with vertical mixing condition in the whole area. In September, nitrate concentration was within 0.52–11.00 μM with stratified condition at Sta. 1 of the western part.

Silicate concentration in the western part in January was lower than that in September,

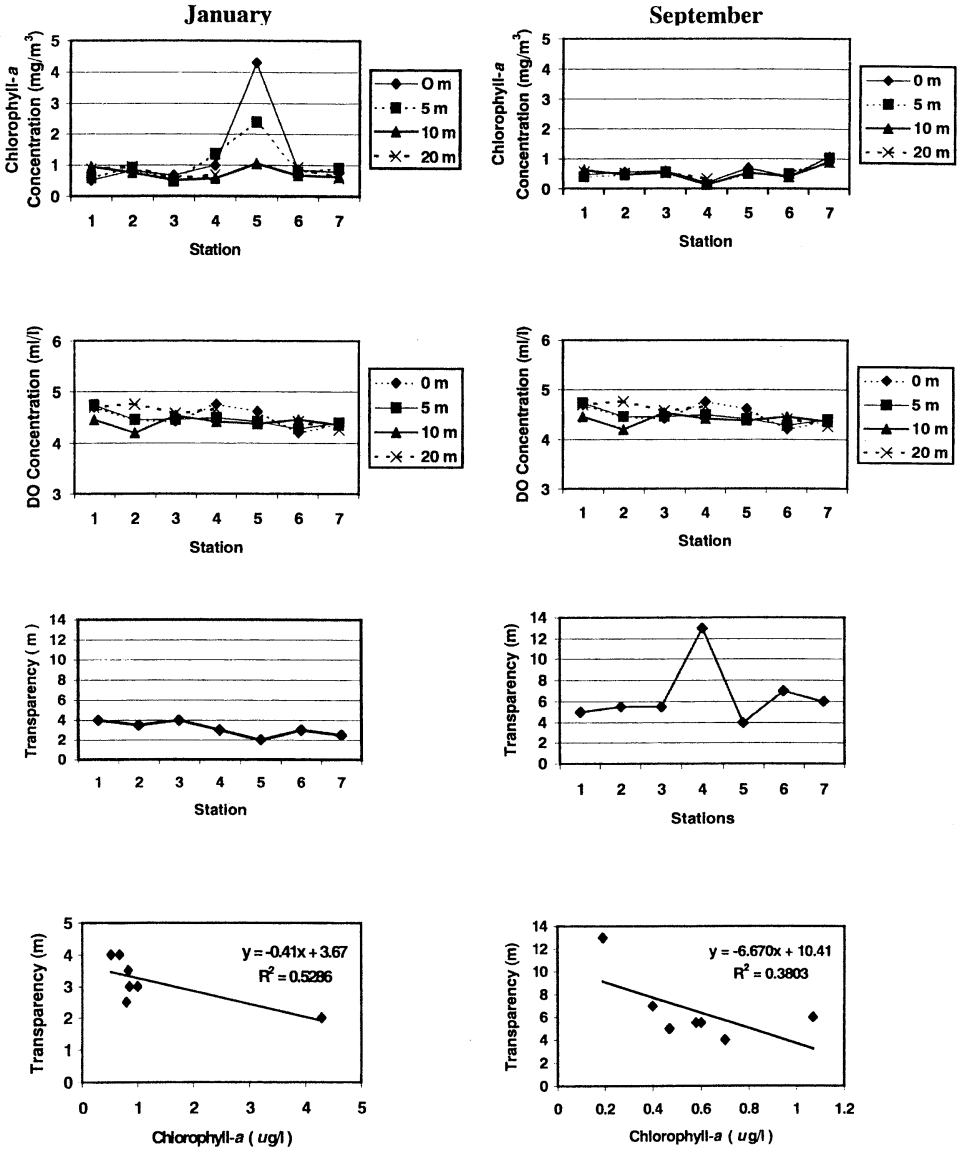

Fig. 4. Horizontal and vertical distributions of chlorophyll-*a* (μ g/l), DO (ml/l)and transparency (m)in the northern coastal area of Java and correlation between chlorophyll-*a* (μ g/l)and transparency (m)in January and September 1981.

except for the surface layer of Sta. 2. While at Sta. 6 of the eastern part, silicate was relatively higher in January than that in September. Silicate concentration was within 1.21–14.54 μ M in January and stratified at Sta. 2 of the western part and Sta. 6 of the eastern part. In September, silicate concentration was within 4.46–12.93 μ M and stratified at Stas. 1 and 3 of the western part and Sta. 5 of the central part.

Moreover, N/P ratio in January was lower than that in September, except for some layers at Stas. 3 and 6. N/P ratio in January was within 0.05–19.00 and in September within 1.75 –22.44.

Horizontal and vertical distributions of chlorophyll-*a*, dissolved oxygen (DO) and water

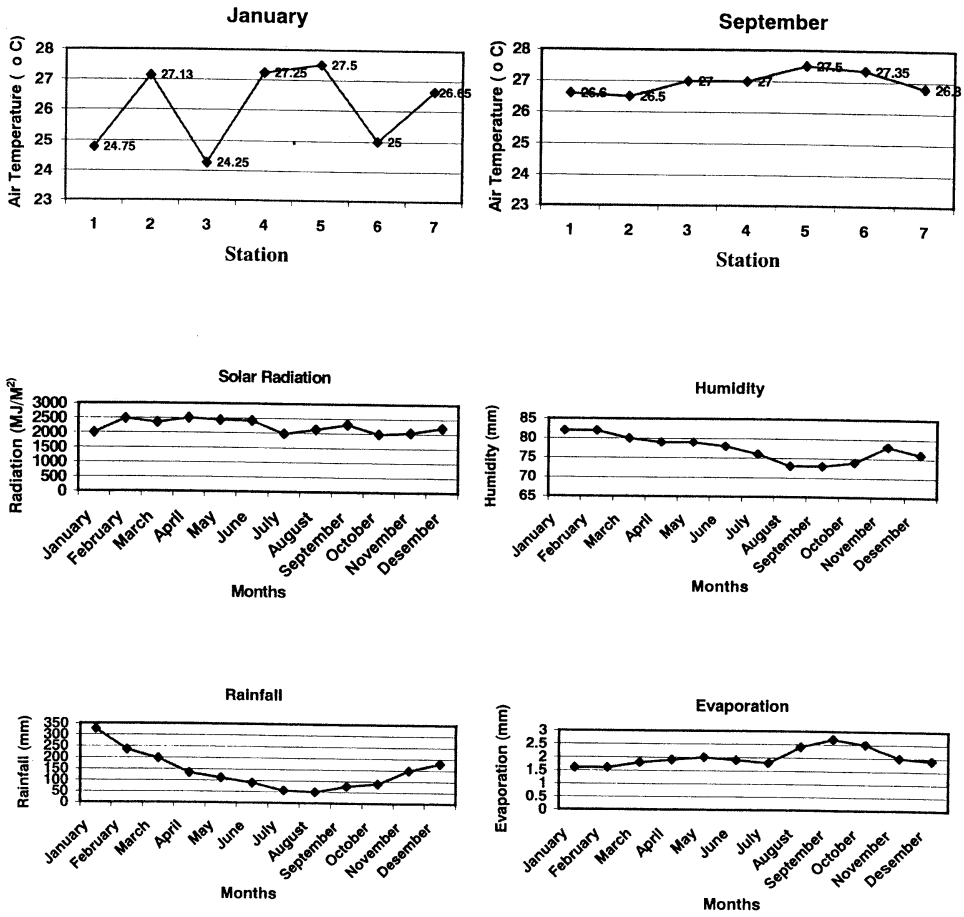

Fig. 5. Air temperature (℃) at the observation stations in January and September 1981, monthly mean solar radiation, rainfall, air humidity and evaporation at Jakarta are derived from the data during 1931–1960 (Meterological Agency, Indonesia).

transparency in January and September 1981 are shown in Fig. 4. Chlorophyll-*a* concentration in January was relatively higher than that in September, especially for Sta. 5 of the central part. Chlorophyll-*a* concentration in January was within 0.54–4.29 μg/l and stratified at Stas. 4 and 5 of the central part. In September, chlorophyll-*a* was within 0.13–1.07 μg/l with vertical mixing condition in the whole area.

DO concentration in the western part in January was slightly lower than that in September. DO concentration in January was within 3.80–4.82ml/l with stratified at Sta. 2 of the western part, Sta. 4 of the central part and Sta. 7 of the eastern part. In September DO concentration was within 4.19 – 4.77ml / l with slightly stratified at Sta. 2 of the western part, Sta. 4 of the central part. Water transparency in January was within 2.0–4.0m and it is lower than that in September within 4.0–13.0m.

4. Discussion

The variability of the water characteristics in the northern coastal area of Java is expected to be affected by meteorological condition, the current of the Java Sea corresponding to the monsoon and local topography of coastal area. Variability of water temperature, salinity and density in the northern coastal area of Java in January (northwest monsoon)and September (southeast monsoon) is caused by precipitation and solar radiation as shown in Fig. 5.

Higher precipitation and lower radiation in January caused water temperature, salinity and density lower than those is September. Higher water temperature in September in due to the stronger solar radiation because the sun crosses the equator southward from the northern hemisphere. This situation was obviously seen on the air temperature status, that is, air temperature in September was higher than that in January as shown in Fig. 5. Other work (ATMADIPOERA *et al.*, 1999) note that the temporal variation of air temperature had a similar pattern to that of the sea surface water temperature.

Lower salinity and density within this region were mainly due to the effect of high river discharge in the rainy season of January as shown in Fig. 5. Lower salinity and density at Stas. 2 and 5 in January were due to high discharge of the Citarum river, the biggest river in the northern coast of West Java, and the Serang river in the central Java, respectively (Fig. 1). Horizontal and vertical distributions of density were governed by those of salinity as shown in Fig. 2. This means that the northern coastal area of Java has a character of estuary.

Horizontal variability of nutrient concentration within this region seemed to be governed by surface current of the Java Sea and precipitation due to the monsoon. This situation was confirmed by TOMASCIK *et al* (1997) which denoted that the concentration of suspended particulate matter (SPM) in the Java Sea was affected by rainfall and surface current of the Java Sea and the condition depended on the distance from shore. For the adijacent area of the shore, the effect of SPM from the terrestrial area is dominant, while the offshore area more than 3km of the shore, the surface current has a significant effect on the horizontal distribution of SPM concentration. NINGSIH and SUPRIJO (1998) denotes that the particulate matter in the Java Sea moves estward in the northwest monsoon and westward in the southeast monsoon. Because the observation areas at this time were located more than 5km from the shore, the effect of the surface current on the horizontal distribution of nutrients within this region will be significant. Moreover, since the concentrations of municipal, agriculture and industrial wastes in the northern coastal area of Java are variously, this situation will also affect on the nutrient distribution. For instance, high concentration of phosphate at Stas. 4 and 5 of central Java in January 1981 was probably due to the addition and accumulation of phosphate by the eastward surface current of the Java Sea that brought a high concentration of nutrient from industrial region of West Java shown in Fig. 1. The accumulation of phosphte in the central part was also occurred due to the presence of the local eddy that was generated by semi-enclosed topography of the central Java as shown in Fig. 1. On the odher hand, higher river discharge of the Serang river in the central Java also contributed on the intensification of such condition. The almost similar pattern was also seen on the distribution of silicate where high concentration was found in the central part and at Sta. 6 of the eastern part in January. High concentration of silicate within this region may be resulted from high discharge of Serang river in the central Java which is added by the eastward surface current into Sta. 6 in the eastern Java. On the contrary, concentration of phosphate and silicate in September was relatively increased toward the western part. It is suspected mainly due to the addition of phosphate from land by the westward surface current, because the river discharge was relatively low during this season. Although the unclear pattern was seen on the variability of nitrate, high nitrate concentration at Sta. 1 of the western Java in September may be related to the addition of nitrate due to the westward current. High concentration of nitrate fund in the lower layer of Sta. 1 in September may be due to high decomposition and demineralization of the organic matter in the bottom layer. Such situation, however, is not supported by the condition of the DO conecentration at that station as shown in Fig. 4. In fact, the DO concentration in the lower layer of Sta. 1 was relatively high. So, more detailed investigation should be conducted to understand the nitrate distribution within this region. Meanwhile N/P ratio within this region shows that nitrate may act as the limiting factor of the primary production in the whole part of the northern coastal area of Java because N/P ratio

is lower than the Redfield ratio of 16.

Variability of chlorophyll-*a* concentration shown in Fig. 4 expresses that chlorophyll-*a* concentration in January was slightly higher than that in September. Higher concentration chlorophyll-*a* at Sta. 2 in the western part and Sta. 5 in the central part in January is probably due to large amount of nutrient supply in the rainy season from the terrestrial environment by increasing river discharge of Citarum river in the western part and Serang river in the central part, respectively. But at Sta. 7 in the eastern part of Java, higher concentration of chlorophyll-*a* in September is suspected to be due to the influence of nutrient and phytoplankton supply from the upwelling area of Banda and Flores Seas (upper panel of Fig. 1) by the westward surface current in the southeast monsoon (TOMASCIK *et al*, 1997). In the central and eastern parts of Java, lower transparency in January is significantly contributed from the phytoplankton bloom generated by increasing nutrient load from the river discharge as supported by the result of correlation analysis shown in Fig. 4.

Variability in dissolved oxygen (DO) was very small. The tendency of the increasing DO toward the eastward in the northwest monsoon and the westward in the southeast monsoon might be related with the primary production variability due to the surface current of Java Sea. Since the DO concentration is governed by not only physical but also bio-chemical processes, the clarification of the DO status within this region should be made in the future by obtaining further information of the main factor of DO variability.

5. Conclusion

The variability of the water temperature, salinity and density in the northern coastal area of Java corresponds to the monsoon which influences in precipitaion, wind and solar radiation. Water temperature in January was lower than that in September as well as for salinity and density.

Nutrients variability, influenced by the local river discharge and the local coastal topography, was also affected by the nutrients transport due to surface current corresponding to the monsoon. Phosphate in the central Java was high in January and that in the western part in September. Silicate was high in the eastern part in January and in the western part in September as well as for nitrate.

Redfield ratio in the whole part of the northern coast of Java is lower than 16, hence, nitrate may act as the limiting factor for the primary production within this region. Chlorophyll-*a* concentration was high in January in the central and western parts due to large supply of nutrients by river discharge. While in the eastern part, higher concentration of chlorophyll-*a* in September may be due to the nutrient supply from the upwelling area in the eastern region of Indonesia by surface current.

The integrated invesitigation of the ecosystem is necessary to be established within this region to understand systematically various factors that influence on the water characteristic for sustainable utilization in the future.

Reference

ATMADIPOERA, A., J. I. PARIWONO and A. SETIAWAN (1999): Physical oceanography of the northeastern Jakarta Bay derived from the coastal monitoring buoy. The Proceeding of 10th PAMS/JECSS, 6–9.

Lembaga Oceanologi Nasional-LIPL (1980): Pemonitoran perairan pantai utara Jawa. Laporan No.1 dan 2. Proyek Penelitian Masalah Pengembangan Sumberdaya Laut dan Pencemaran Laut. Kantor Menteri Negara Pengawasan Pembangunan dan Lingkungan Hidup dan Lembaga Oceanologi Nasional-LIPI.

Lembaga Oceanologi Nasional-LIPL (1981): Pemonitoran perairan pantai utara Jawa. Laporan No.3 dan 4. Proyek Penelitian Masalah Pengembangan Sumberdaya Laut dan Pencemaran Laut. Kantor Menteri Negara Pengawasan Pembangunan dan Lingkungan Hidup dan Lembaga Oceanologi Nasional-LIPI.

NURDJANA, M. L. (1997): Development of shrimp culture in Indonesia. Papers presented at Bangkok FAO Technical Consultation for Sustainable Shrimp Culture. FAO Fisheries Report No.572, Supplement, 68–76.

NINGSIH, N. S. and T. SUPRIJO (1998): Particle trajectory simulation in Java Sea generated by tide and wind driven criculation using a three dimensional ocean model. Journal Teknik Sipil, Vol.5, No.3, 153–159.

ONGKOSONO, O. S. R. *et al*., (1990): Kualitas pesisir dan lautan. In: Kualitas lingkungan di Indonesia 1990

(S. T. Djajadiningrat. ed.): 197–233. Kant. Meneg. KLH, Jakarta.

ONGKOSONO, O. S. R. (1992): Human activities, environmental problems and management of the northern coast of West Java, Indonesia, with emphasisthe Jakarta Bay. Unesco reports in marine scienc: Coastal systems studies and sustainable development. Proceeding of the COMAR Interregional Scientific Conference UNESCO, Paris, 21–25 May 1991, UNESCO, 99–124.

PARSON, T. R and J. D. H. Strickland (1963): Discussion of spectrophotometric determination of marine plant pigments with revised equation for ascertaining chlorophylls and carotenoids. J. Mar. Res., **21**, 155–163.

PRASENO, D. P. (1995): Notes on mass mortality of fish in Jakarta Bay and shrimp on brackish water pnds of Kamal, Jakarta. Proceeding ASEAN Canada Midterm Review. Conference on Marine Science. Singapore 24–28 October 1994, 348–350.

PRASENO, D. P. and Q. ADNAN (1996): Phytoplankton community and abundance in some estuaries in the northern coast of Java. Proceeding of Making Efficient Use of Technology Application on Marine Environmental Monitoring for Supporting Sustainable Development. Directorate for Human Settlement and Environmental Technology. Agency for the Assessment and Application of Technology and OCEANOR Norway, 1–10.

PUTRI, M. L. *et al.* (1999): Characteristic of tidal and wind current in Jakarta Bay. Proceeding International Seminar on Application of Seawatch Indonesia Information System for Marine Resources Development. Directorate for Environmental Technology. Agency for the Assessment and Application of Technology and Oceanographic Company of Norway Asia, 150–162.

ROHILAN, L. (1992): Keadaan sifat fisik dan kimia perairan di pantai zona industri Krakatau Steel, Cilegon. Fakultas Perikanan. Institut Pertanian Bogor. 106pp.

STRICKLAND, J. D. H. and T. R. PARSONS (1968): Practical handbook of sea water analysis. Fis. Res. Board Canada Bull., No.167, 1–1311.

SACHOEMAR, S. I. and T. YANAGI (1999): Seasonal variation in water quality at the northern coast of Karawang-West Java, Indonesia. La mer, **37**, 91–101.

TOMASCIK, T., A. J. MAH., A. NONTJI and M. K. MOOSA (1997): The ecology of Indonesian seas. Part I , Vol.VII, Periplus Editions (HK) Ltd. 642pp.

U. S. Navy Hydrographic Office (1959): Introduction manual for oceanographic observation. U. S. Navy Hydrogr. Off., Pub. 607, 1–210.

Received July 10, 1999
Accepted December 5, 2000

La mer 39 : 87–93, 2001
Société franco-japonaise d'océanographie, Tokyo

画像解析システムを用いた二枚貝幼生の自動識別法の試み

寺崎　誠*・浜口正巳**・薄　浩則**・石岡宏子***

Automated identification of larval bivalves utilizing an image processor

Makoto TERAZAKI*, Masami HAMAGUCHI**, Hironori USUKI** and Hiroko ISHIOKA***

Abstract : The possibility of automated identification of larval bivalves, especially a short-necked clam (*Ruditapes philippinarum*) from other zooplankton occurred in the Seto Inland Sea, was examined by utilizing an image processor. Before image analyses, pre-sorting between larval bivalves and other zoopalnkton with different mesh sizes and salinity gradient. The aspect ratio(maximum length/maximum breadth), roundness shape factor[RSF: (maximum length^2 /area) × (π/4)] and unevenness shape factor[USF:(perimeter/area)×4π] of larval bivalves, copepods, chaetognaths, polychaeta, ostracoda and appendicularian, were measured. An operation combining the aspect ratio, RSF and USF was very effective for sorting and identification of larval valves. The special software (NIRECO Co. Ltd.) for the pattern recognition of rice grain shape was also used in order to distinguish clearly a short-necked clam from other laraval bivalves.

Key words : *identification, zooplankton, bivalve, image processor*

1. はじめに

内湾や沿岸域で重要な水産生物であるアサリ（*Ruditapes philippinarum*）などの二枚貝の資源を管理する上で，産卵直後の初期生態の調査は不可欠である。二枚貝の幼生は着底するまでは浮遊生活を営み，従来，沿岸域で二枚貝の初期生態を調査するためにはポンプ，プランクトンネットが用いられるが，内湾，沿岸ではカイアシ類，枝角類，珪藻，渦鞭毛藻などのプランクトンや非生物が同時に採集されるため，選別作業には多大な労力と時間が必要であった。

1980年代の後半より画像解析システムを利用して植物プランクトン（UHLMAN *et al.*, 1978; ISHII *et al.*, 1987; 辻・西川, 1981 ; TSUJI and NISHIKAWA, 1984），動物プランクトン（JEFFRIES *et al.*, 1984; TERAZAKI and ISHII, 1986 ; 寺崎, 1990 ; 角井, 1998）を自動識別する研究が行われるようになった。カイアシ類などの甲殻類では孵化後，成長過程で変態を行い，形態の変化も大きいが，それに比べると二枚貝の幼生の成長に伴う外部形態の変化は小さく，画像解析システムによる形状認識の可能性は大きい。本研究では内湾でプランクトンをポンプ採取後，篩を用いたサイズ別区分，塩分勾配（比重差）を用いた分別などの前処理を施した後，高速画像解析システムによる形状識別によりアサリ幼生のみを自動的に選別することを目的とした。

* 東京大学海洋研究所　〒164-8639　東京都中野区南台1-15-1 Ocean Research Institute, University of Tokyo, 1-15-1 Minamidai, Nakano, Tokyo 164-8639, Japan
** 瀬戸内海区水産研究所　〒739-0452　広島県佐伯郡大野町丸石2-15-5 National Research Institute of Fisheries and Environment of Inland Sea, 2-17-15 Maruishi, Ohno, Saeki, Hiroshima 739-0452, Japan
*** 養殖研究所　〒516-0193　三重県度会郡南勢町中津浜浦422-1 National Research Institute of Aquaculture, Nansei, Mie 516-0193, Japan

2. 研究方法

1）試料の前処理方法の検討

ア）篩を用いたプランクトンのサイズ区分

1995年10月，南西海区水産研究所近くの宮島長浦の5 m層よりポンプを用いて500Lの海水を採水し，画像解析を効率よく行うため前処理として5つの目合いの異なる篩（4 mm，2 mm，0.5 mm，250 μm，63 μm）を用いて区分した後，5％海水ホルマリンで固定した。各区分ごとに顕微鏡下で出現したプランクトンの分類と計数を実施した。

Table 1. Number of individuals of each zooplankton (per 500 L) collected from Nagaura, Seto Inland Sea with different mesh-size net.

mesh-size (mm)	collected zooplankton (inds./500L)
2-4	Chaetogantha (*Sagitta enflata*)-1
1-2	Ctenophora-2, Polychaeta-1
0.5-1	Copepoda (*Acartia*)-2, Copepoda (*Oithona*)-1
0.25-0.5	Copepoda-75, Copepoda larvae-11, Appendicularia-2, Radioraria-1, Ctenophora-1, Bivalve larvae-1
0.063-0.25	Copepoda larvae-680, Bivalve larvae-152, Polychaeta-56, Cladocera-17, Cirripedia larvae-10, Chaetognatha larvae-4, Shrimp larvae-2, Ctenophora-1, Radioraria-1

イ）塩分勾配による分別実験

プランクトンネットによって採集されたカイアシ類および南西海区水産研究所で飼育されたアサリ幼生を用いて，生息環境の塩分条件を変えた時の鉛直分布構造の経時変動を調査した。実験には容量 50 cc，深さ 15 cmの円筒ガラスシリンダーを用いた。塩分を 29.1 PSU，23.3，17.5，14.6 の 4 条件に設定し，水温 22 度で孵化後 16 日目のアサリ幼生を 200 個体ずつ，カイアシ類の場合は宮島長浦より目合 0.1 mmのネットで採集された生体を 4 時間，暗条件下で飼育しその後 20 個体ずつ上記 4 条件の塩分に設定した円筒シリンダーに入れ，暗条件下で 5 分，10 分，15 分，30 分，60 分および120分後の鉛直分布構造を調べた。

2）高速画像解析システムを用いた計測

高速画像解析システム「ルーゼックス-FS」（ニレコ製）を用いて瀬戸内海より採集された動物プランクトンおよび二枚貝幼生の最大長，縦横比，丸さの度合い（RSF：最大長の 2 乗×π/面積×4），凹凸の度合い（USF：周囲長/面積×4π）を計測した。計測には各種類 10 個体を用いた。

さらにニレコ（株）の開発した米の形状解析ソフトを用いてアサリ幼生（D－5，D－10，D－15，D－20），ヒメアサリ（*Ruditapes variegata*），ホトトギス（*Musculus senhausia*），ムラサキイガイ（*Mytilus edulis*），イガイ（*Mytilus coruscus*），マガキ（*Crassostrea gigas*）およびカイアシ類幼生についての形状識別を試みた。解析試料数は 1 視野 1 試料とし，顕微鏡写真をマクロスタンド及びCCDカメラにより入力した。このソフトの原理は一次元フーリエ変換で試料の輪郭は 256 画素以上あるような倍率に設定し，二値画像よりその輪郭座標を得て重心からの距離をフーリエ解析し，データベースに書き込み，最終的にはグラフィック表示した。重心を中心に外部輪郭を 128 分割した時に得られる輪郭片の凹凸を 0（直線）から 20 以上に区分した各頻度を求め，結果は最大の区分を 100 としてそれぞれの相対値を棒グラフで示した。計測には各種類およびアサリ幼生の成長段階ごとに 10 個体を使用した。

3. 結　果

1）篩を用いたプランクトンの分別

篩による分別では 1 mm 以上にはクラゲ類，ごかい，矢虫類，0.5 mm 以上には *Acartia*, *Oithona* などのカイアシ類，250 μ 以上にはカイアシ類，尾虫類，クラゲ幼生，放散虫などが見られ，対象生物の二枚貝幼生は 63-250 μm の範囲に含まれ，この区分には枝角類，フジツ

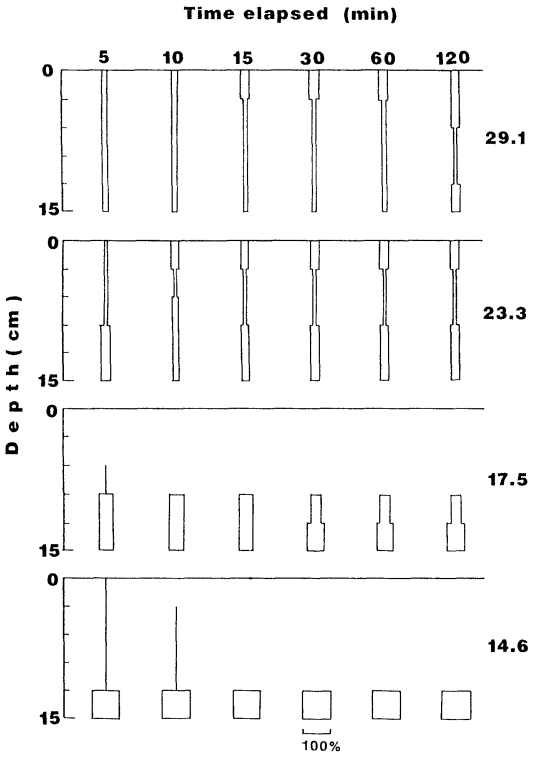

Fig. 1. Time-series vertical distribution of a short-neked calm larvae under different salinity conditon.

ボ幼生，*Microsetella* のような小型カイアシ類が検出された（Table 1）。

2）塩分勾配を用いた分別

原海水（塩分 29.1 PSU）の入ったシリンダー内ではアサリ幼生（密度：16 個体/cc）は上下層に均等に分布しこの状態は塩分 23.3 に下げても保たれるが，塩分 17.5 以下では 10 分以内にすべての個体は底層に沈降した（Fig. 1）。一方，現場に多く生息するカイアシ類は塩分 14.5 まで下げてもかなりの個体が上層に滞泳していた（Fig. 2）。

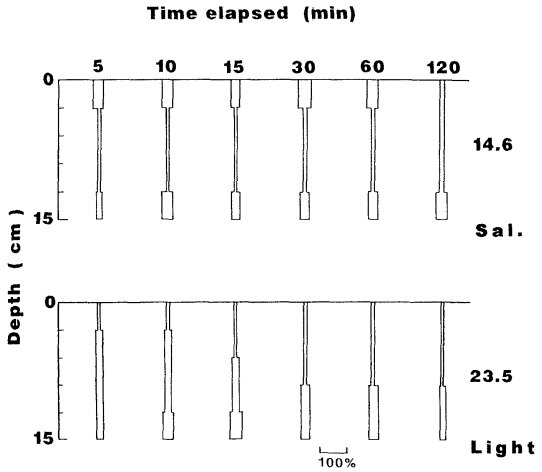

Fig. 2. Time-series vertical distribution of small copepoda, *Oithona* under low salinity (14.6 PSU) and strong light (23.5 μmol・m^{-2}・S^{-1}) condition.

3）高速画像解析システムによる計測

マガキ，アサリの幼生の縦横比および形状計数は瀬戸内海から採集されたカイアシ類，矢虫類，尾虫類，ゴカイ類などの動物プランクトンの計測値とは大きく異なり（Table 2），アサリ幼生（178–214 μm）の縦横比は平均 1.11，形状係数は平均 1.19，カキ幼生（158–275 μm）では縦横比，形状係数の平均はそれぞれ 1.12，1.23 で両者の値はアサリのほうが僅かに小さい傾向がある。しかし *Oithona*, *Acartia* のようなかいあし類では縦横比は 1.3 以上，形状係数は 4 以上で二枚貝幼生とは大きな差異が認められた。

アサリ幼生の縦横比，丸さの度合いは成長に伴い小さくなる傾向があり，凹凸の度合は成長段階によって異なった（Fig. 3）。瀬戸内海に出現するマガキ，ヒメアサリ，ホトトギスとアサリの幼生の縦横比，形状係数（丸さの度合いおよび凹凸の度合）を比べると，3 つの特性値を組み合わせる事により識別可能であるが，ホトトギス幼生は形状が大変類似しているので，他の方法を検討する必要があった（Fig. 4）。

外部輪郭線の微妙な差異の識別に用いられる「米の形状解析ソフト」を使用したアサリ幼生，他の貝およびカイアシ類幼生の形状解析の結果，カイアシ類幼生は凹凸の頻度が貝類に比べて高く，貝類とは明確に区別できた。またアサリ幼生とマガキ，ヒメアサリ，ホトトギスなど他の貝の幼生とも表示されたグラフのパターンの違いを比較することにより，区別が可能であったが（Fig. 5），対象生物のアサリ自身，発育に伴い形状が若干変化することも明らかになり（Fig. 6），ホトトギスはアサリのD–5 幼生の輪郭と類似していた。

4. 考　察

瀬戸内海には小は珪藻，渦鞭毛藻，繊毛虫，カイアシ

Table 2. Body Length, Aspect Ratio and Roundness Shape Factor of zooplankton occurred in the Seto Inland Sea.

Taxa of zooplankton	Body Length(mm)	Aspect Ratio	Roundness Shape Factor
Copepoda			
Acartia sp.	0.6	1.37	5.5
Oithona sp.	0.5	1.71	4.39
Chaetogantha			
Sagitta enflata	11.2 –29.6	5.14(1.7)	8.78(0.95)
S. crassa	7.5 –11.6	5.62(0.82)	9.15(0.53)
Appendicularia	2.1 – 8.9	4.32(1.00)	5.99(1.72)
Polychaeta	6.0 –20.9	2.53(0.79)	4.92(2.42)
Ostracoda	2.4 – 3.2	1.60(0.19)	1.72(0.15)
Bivalve larvae			
Ruditapes philippinarum	0.18– 0.21	1.11(0.06)	1.19(0.07)
Crossostrea gigas	0.16– 0.28	1.12(0.08)	1.23(0.09)

Note: Figures in the parenthesis show standard deviation.

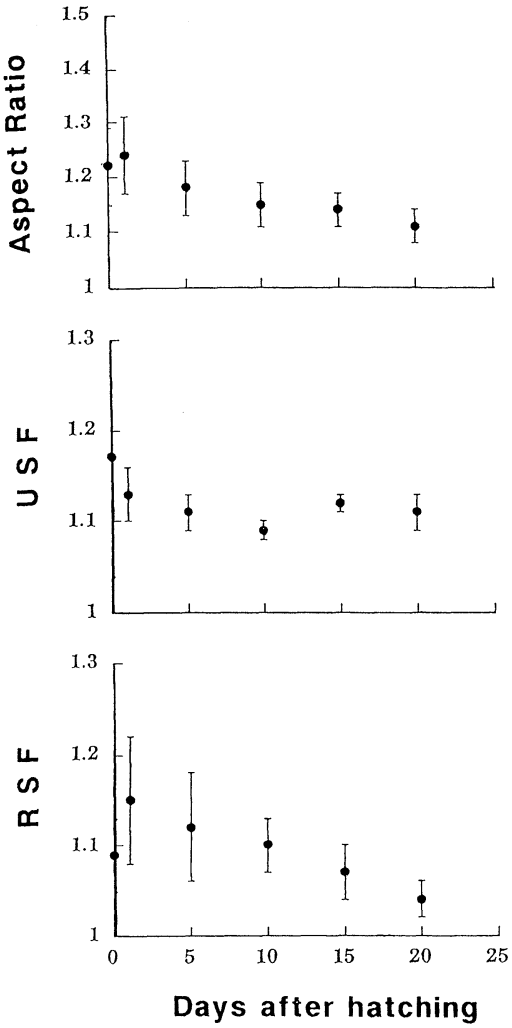

Fig. 3. Aspect ratio, RSF and USF of a short-necked clam in each developmental stage.

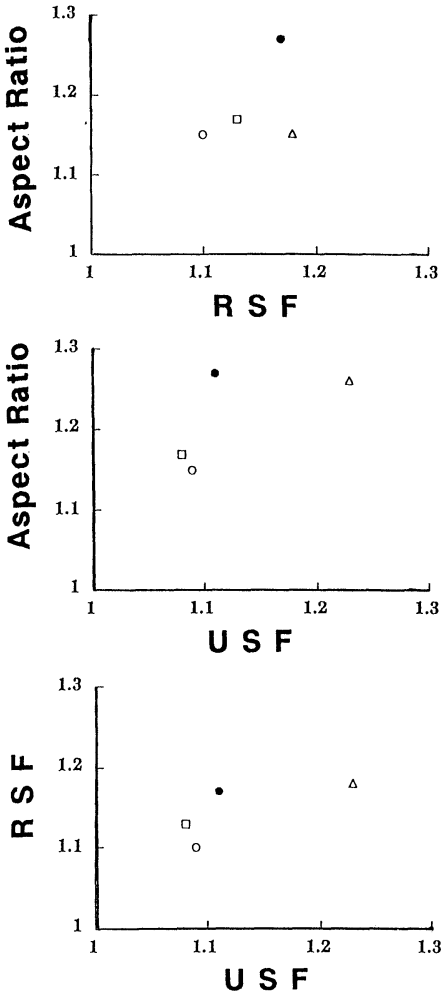

Fig. 4. Correlation of three parameters(Aspect ratio, RSF and USF)of larval bivalves occurred in the Seto Inland Sea: *Ruditapes philippinarium* (○), *R. variegata* (●), *Musculus senhausia* (□) and *Crassostrea gigas* (△).

類幼生から大はミズクラゲ，矢虫，稚仔魚など様々なプランクトンが生息し，時には赤潮も形成される（岩崎，1976；山口，1998)。この海域にはマガキ，ホトトギス，イガイ，ムラサキイガイ，アサリ，ヒメアサリなどの多くの貝類も生息しているが，これらの貝類は孵化後しばらく海中を浮遊し，やがて着底する。着底時期および大きさは種類によってことなるが，アサリの場合，22 ℃では受精後 5 時間で繊毛を生じて回転運動をはじめ，10 時間で担輪子となり 22 時間で有殻仔貝となり殻長 200–230 μm，殻高 190–220 μm に達した時に着底する。実験に使用した瀬戸内海区水産研究所で飼育しているアサリ幼生は孵化後約 20 日でこの大きさに達する（Fig. 7)。有用水産資源であるアサリの資源調査をするためには，浮遊期間にプランクトンネットあるいはポンプで採集して生物量を把握する必要がある。この時，問題になるのは同時採集される植物プランクトン，カイアシ類，枝角類，甲殻類幼生などが多量に出現するため，画像解析の手法を使う前に迅速にアサリを含む貝幼生を分離する必要がある。植物プランクトンの場合には，細胞内に葉緑素があるので，蛍光顕微鏡などを利用して他生物や非生物との分離は容易であるが（Furuya and Marumo, 1983)，動物プランクトンの場合には有効な前処理が必要となる。なるべく対象生物に他の者が混じらないような条件で画像処理した方が処理時間も短く，かつ精度も良い（寺崎，1990)。

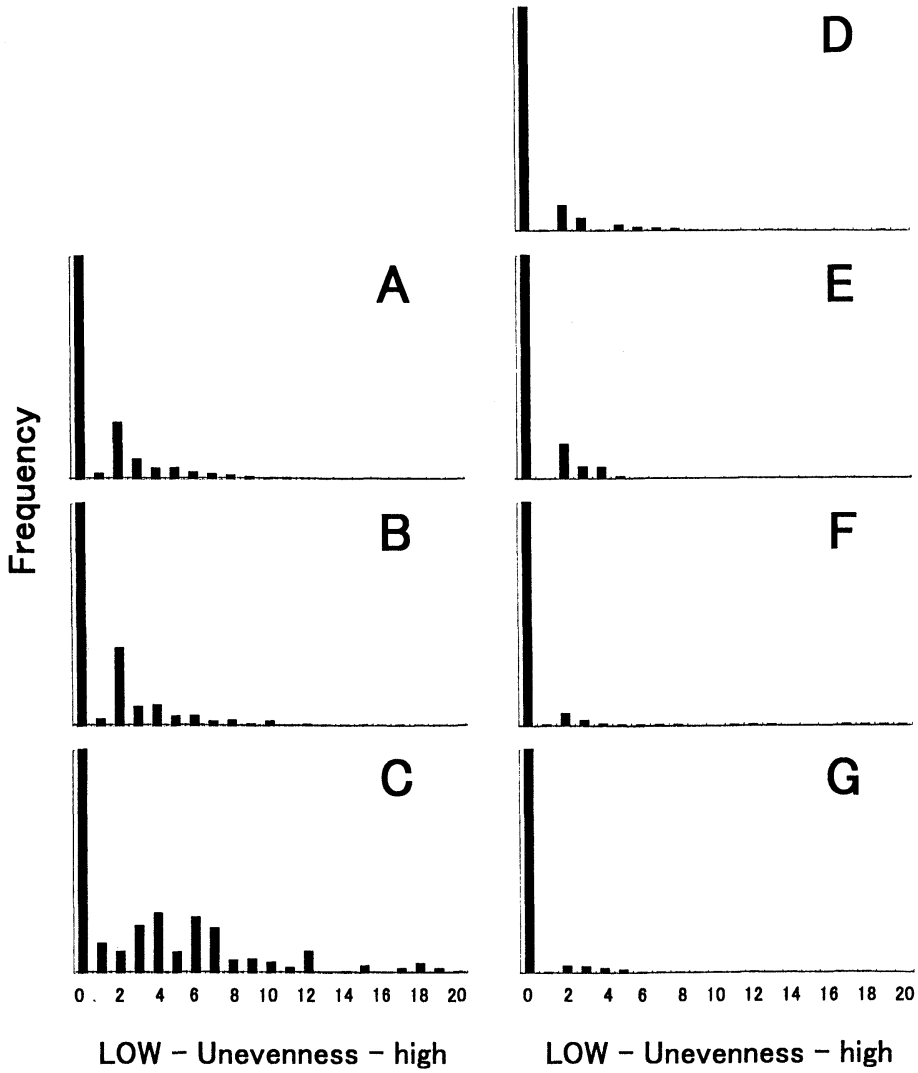

Fig. 5. Unevenness frequency distribution of external border line of larval bivalves and copepoda larvae: A-*Mytilus edulis*, B-*M. coruscus*, C-Copepoda larvae, D-*Crassostrea gigas*, E-*Ruditapes variegata*, F-*Musculus senhausia*, G-*Ruditapes philippinarium*(D-15 stage).

本研究では篩による第一段階の処理を行った後で，塩分に対する順応能力の差異を利用して動物プランクトンの中から二枚貝幼生の摘出を試みた。二枚貝幼生はほとんど63-250μmの区分に含まれるので，篩による分別は有用であった。しかしこの区分には幼生の他に小型カイアシ類，ゴカイ，枝角類などが多く出現したため，第2段階で異なった塩分濃度の条件下で飼育すると貝幼生はカルシウムで形成される硬い殻を持つため，カイアシ類，枝角類などの甲殻類に比べて，体比重も重く，遊泳力も小さいため，塩分濃度を徐々に低くすることにより時間とともにアサリ幼生は沈降する傾向が明らかになり，この手法で両者の大まかな分離が可能となった。

篩および塩分勾配を利用した前処理により，二枚貝幼生と分離できなかった小型カイアシ類の一部が，画像解析用試料として残される。甲殻類は発育により変態を行い，かつ見る姿勢（方向）によって形態が異なるため，画像解析による識別が困難な場合があるが（寺崎，1987，1990），二枚貝幼生は坦輪子を除き体が扁平で，麻酔やホルマリンなどで固定した時に横向きの姿勢になり，かつ外部輪郭の凹凸が少ないので，画像解析システムを用いた認識は他の生物に比べて容易で，誤査定も少ない。二枚貝幼生とカイアシ類，ゴカイ，矢虫類，枝角類など

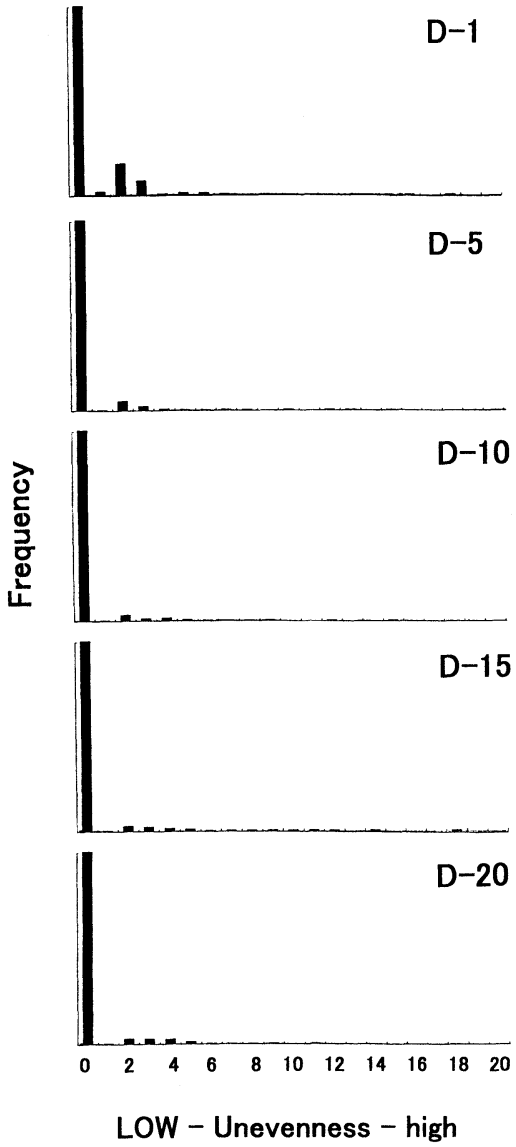

Fig. 6. Unevenness frequency distribution of external border line of a short-necked clam larvae in each developmental stage.

の動物プランクトンとの識別は縦横比，凹凸の度合，丸さの度合いなど複数の特性値を組み合わせることにより可能である。しかし，ヒメアサリ，ホトトギスなど形態が類似している場合には，今回用いたような特別のソフト（米の形状解析）の併用も不可欠である。

海洋の動物プランクトンの中には，赤，オレンジ，黒，青など様々な色を帯びているものも多く，画像解析の手法では微妙な色調の差異の認識も可能である。対象生物のアサリ幼生は無色であるが，免疫学的方法で着色することができれば，他の生物との識別も特性値やソフトを使用しなくても容易にできる。

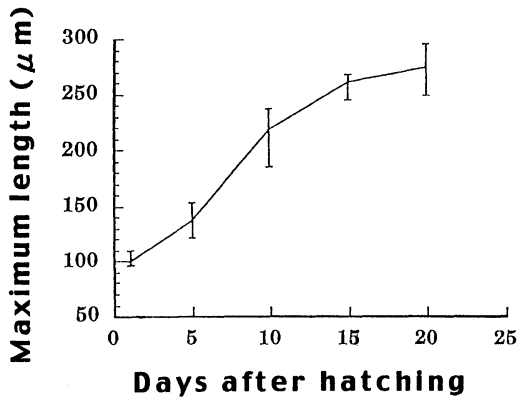

Fig. 7. Growth curve of short-necked clam larvae.

しかし，アサリ幼生自体も孵化後の発育に伴い形態が変化するので，この点も将来検討する必要がある。

謝　辞

本研究を遂行するにあたり「米の形状解析ソフト」の使用方法をご教示いただいた株式会社ニレコの田辺寛一郎課長，臼井　修主任に深甚なる謝意を表します。また，始終，激励をいただいた瀬戸内海区水産研究所森岡泰啓部長に深く感謝致します。本研究は農林水産技術会議の特別研究「魚介類の初期生態解明のための種判別技術の開発」の一環として行われた。

文　献

ISHII, T., R. ADACHI, M. OMORI, U. SHIMIZU and H. IRIE (1987): The identification counting and measurement of phytoplankton by an image-processing system. J. Cons, In. Explor. Mer. **43**, 253-260.

岩崎英雄（1976）：赤潮－その発生に関する諸問題．海洋出版，東京，126頁.

FURUYA, K. and R. MARUMO(1983): Size distribution of phytoplankton in the western Pacific Ocean and adjacent waters in summer. Bull. Plankton Soc. Japan, **30**, 21-32.

JEFFRIES, H. P., M. S. BERMAN, A. D. POULARIKAS, C. KATSINIS, I. MEALS, K. SHERMAN and L. BIVINS (1984): Automated sizing, counting and identification of zooplankton by pattern recognition. Mar. Biol., **78**, 329-334.

角井嘉美（1998）：沿岸海域における浮遊生物組成把握のための計測システム，p.1474-1479，沿岸の環境圏（平野敏行監修），フジテクノシステム，東京.

寺崎　誠（1987）：画像解析法によるプランクトン研究．沿岸海洋研究ノート，**24**，99-105.

寺崎　誠（1990）：プランクトンのパターン認識．日本

海洋理工学会誌，**2**，49–55.
TERAZAKI, M. and T. ISHII(1989): Examination of the possibility of automated identification of chaetognata utilizing an image processor. Bull. Plankton Soc. Japan, **33**, 95–100.
辻 尭・西川 孝（1981）：画像処理による細胞レベルの微生物量の測定：2．従来の測定法法の問題点と画像処理による克服．化学と生物，**19**，268–274.
TSUJI, T. and T. NISHIKAWA(1984): Automated identification of red tide phytoplankton *Prorocentrum triestinium* in coastal areas by image analysis. J. Oceanogr. Soc. Japan, **40**, 425–431.
UHLMAN, D. O. SCHIMPERT and W. UHLMAN(1987): Automated phytoplankton analysis by a pattern recognition method. Int. Rev. ges. Hydrobiol., **63**, 575–583.
山口峰生（1998）：赤潮，P181–190，沿岸の環境圏（平野敏行監修），フジテクノシステム，東京.

2000年6月14日　受付
2001年4月23日　受理

La mer 39 : 95–106, 2001
Société franco-japonaise d'océanographie, Tokyo

Oceanic structures in the vicinity of Komahashi Daini Kaizan, a seamount in the Kyushu-Palau Ridge Part I. Temperature and salinity fields

Yoshihiko SEKINE*

Abstract : Hydrographic observations by use of CTD and ADCP in the vicinity of a seamount, Komahashi Daini Kaizan, located in the Kyushu-Palau Ridge, were carried out six times from 1989 to 1993. Results of the observed temperature and salinity fields are presented in this paper, as a Part I of this study. Various kinds of vertical shift of isotherms, isohalines and isopycnals are observed around the seamount. It is also shown that the less saline water less than 34.2 psu corresponding to the North Pacific Intermediate water is not observed over the top of this seamount, while the less saline water is observed off the topography of the seamount, which is due to enhanced vertical mixing by the internal wave over the top of seamount and/or the topographic effect of the seamount which forces a less saline water to flow along isopleth of depth of the seamount. In July 1989, the siginificant changes in the temperature and salinity fields are observed during only one week by the approach of small meander of the Kuroshio generated in southeast of Kyushu. Almost estimated Rossby heights (fL/N) are smaller than the peak depth of the seamount (289 m), and the observed height of the baroclinic Taylor column evaluated from the vertical displacement of isotherms and isohalines does not reach to the surface layer, both of which shows that the topographic effect of the seamount does not reach to the sea surface.

Key words : *Komahashi Daini Kaizan, North Pacific Intermediate water, sea mount*

1. Introduction

In the northern Philippine Basin, there have been several observations on the topographic effect of seamount. FUKASAWA and NAGATA (1978; 1980) observed the oceanic structure near the Shoal Kokushou-sone located in southwest of Kyushu. Upwelling along the northern slope of the shoal was shown by the temperature observation (FUKASAWA and NAGATA, 1978), while upwelling along southern slope was detected in June 1977 (FUKASAWA and NAGATA, 1980). Furthermore, FUKASAWA (1983) suggested that distribution of isothermal layers is a helpful indicator of the nature of oceanic structures in the vicinity of the shoal Kokushou-sone. SEKINE and MATSUDA (1987a, b) made hydrographic observations over a bump Tosa-Bae off Shikoku south of Japan (Fig. 1a). They observed a cold eddy west of this bump and a warm eddy east of it. In the later observations (SEKINE *et al.*, 1994), salinity minimum water was found on the northern side of the Tosa-Bae, which suggested the westward intrusion of less saline water over the northern slope. KONAGA and NISHIYAMA (1978) and KONAGA *et al.* (1980) observed that a cold eddy detached from the Kuroshio large meander was trapped over a seamount, the Daini Kinan Kaizan (Fig. 1a). SEKINE and HAYASHI (1992) observed that vertical shift of isotherm and isohaline above the top of the seamount, Daini Kinan Kaizan (Fig. 1a) was maintained more than 10 days, which suggested that the vertical shifts of the isotherm and isohaline are rather stable.

In the present study, oceanic structures over the seamount "Komahashi Daini Kaizan (Fig. 1a) are studied by use of the observational data of six cruises (Table 1). The Komahashi Daini

* Institute of Oceanography, Faculty of Bioresources, Mie University, 1515 Kamihama, Tsu, Mie, 514-8507 Japan

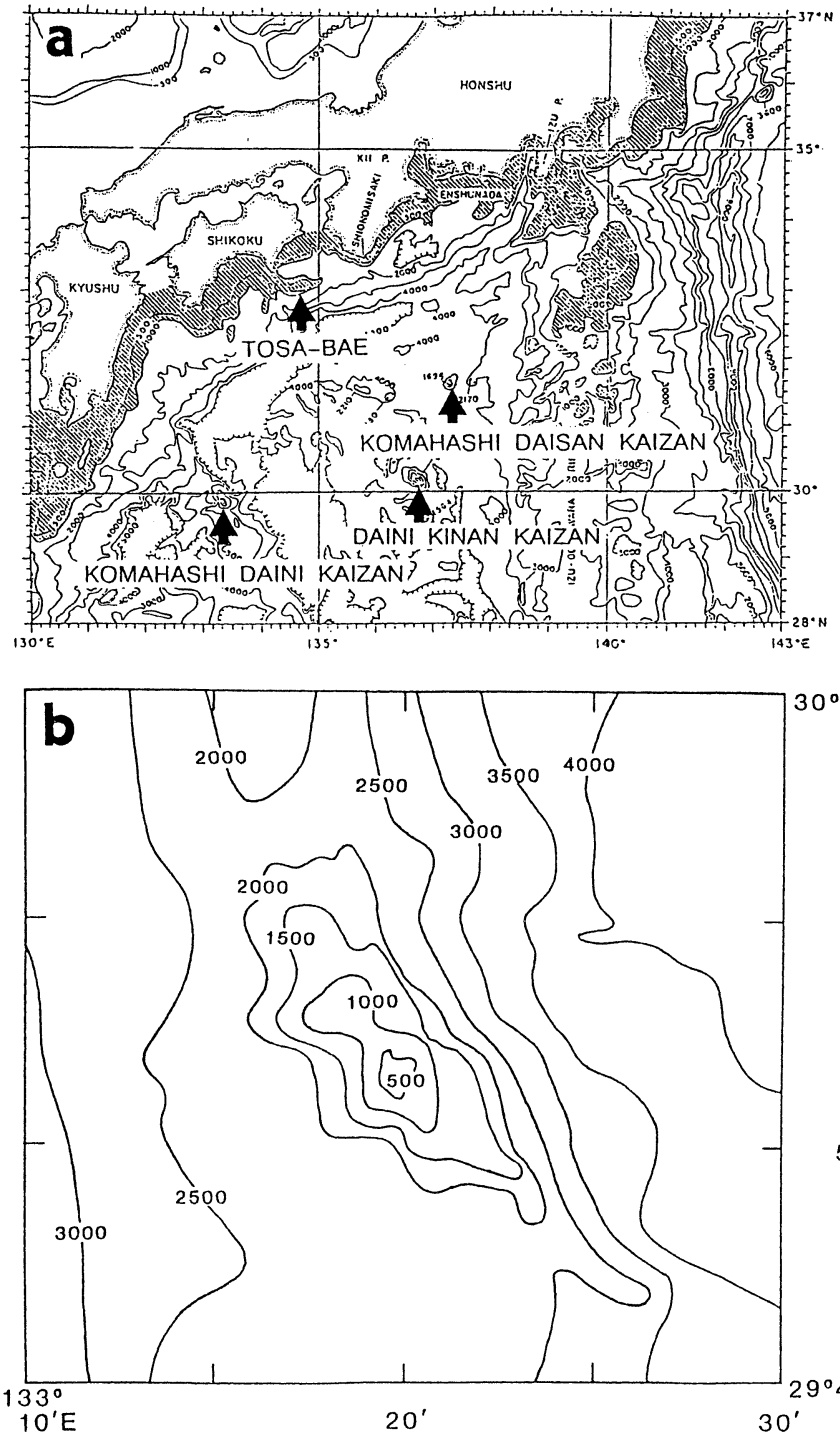

Fig. 1. (a). Location of the seamount "Komahashi Daini Kaizan" and other seamounts south of Japan. Isopleths of depth (in meter) are also shown (after TAFT, 1972). (b) Bathymetry in the vicinity of the Komahashi Daini Kaizan.

Table 1. Hydrographic observations around Komahashi Daini Kaizan.

Cruise Name	Periods of Observation	Obsercvational line	Main instruments
KS-89JUL1	14-16 Jul. 1989	**a, b**	CTD and ADCP
KS-89JUL2	22-24 Jul. 1989	**c, d, e**	CTD and ADCP
KS-89DEC	5- 7 Dec. 1989	**f, g**	CTD and ADCP
KS-90MAY	19-21 May. 1990	**h**	CTD and ADCP
KS-90JUL	13-14 Jul. 1990	**i, j, k**	Mi-com. BT
KS-93JUL	16-17 Jul. 1993	**l, m**	CTD, XBT and ADCP

Kaizan is located in the Kyushu-Palau Ridge. This seamount has an elliptic shape (Fig. 1b), of which 1000 m isopleth has a long axis of about 8 km from southeast to northwest and a short axis of about 4 km from southwest to northeast. The depth at the peak of this seamount is 289 m. In periods of a small meander path of the Kuroshio off Kyushu (SHOJI, 1972; SOLOMON, 1978; SEKINE and TOBA, 1981), the main axis of the Kuroshio approaches to this seamount. It is noted that there have been no detailed hydrographic observations over this seamount. Therefore, we have made six hydrographic observations in its vicinity by use of the training vessel "Seisui-maru" of Mie University (Table 1). I present the results of the observed temperature and salinity in this paper, as a Part I of this study. As for the velocity fields, I will present it in Part II (SEKINE, 2001) of this paper.

2. Observations

In six observations (Table 1), temperature and salinity were observed mainly by CTD. Accuracy of temperature and salinity is 0.01 ℃ and 0.05 psu, respectively, the latter of which is checked by the salinometer (Model 601 MKIII).

Main paths of the Kuroshio during the observational periods are shown in Fig. 2. A small Kuroshio meander off Kyushu was formed in July 1989, while the Kuroshio path was located relatively far from the seamount in the other

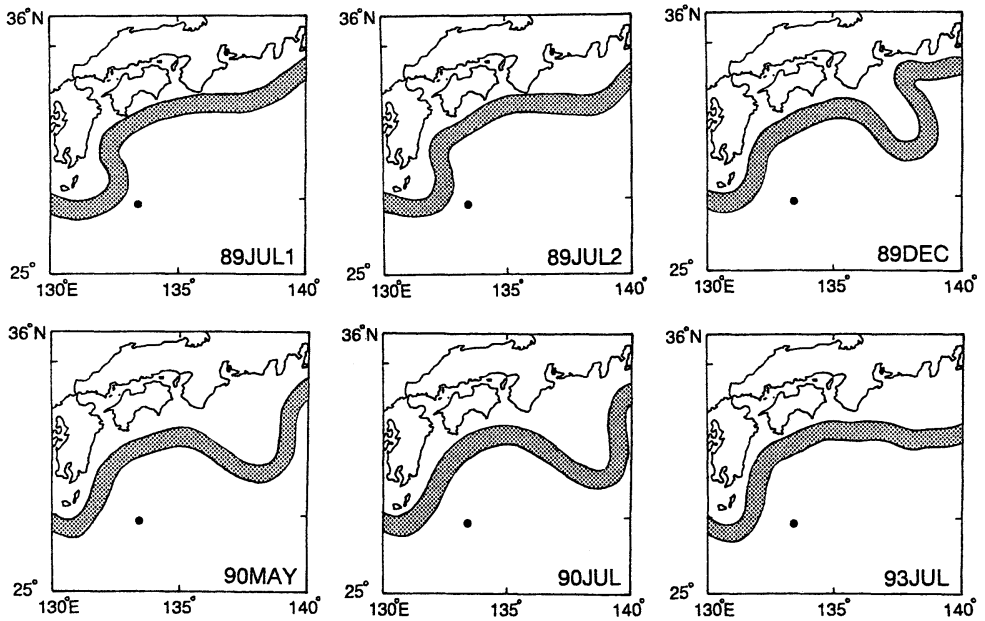

Fig. 2. Main Kuroshio path during the six observation basing on the Prompt Report of Oceanic Condition compiled by Maritime Safety Agency (stippled band) and the location of the Komahashi Daini Kaizan (closed mark).

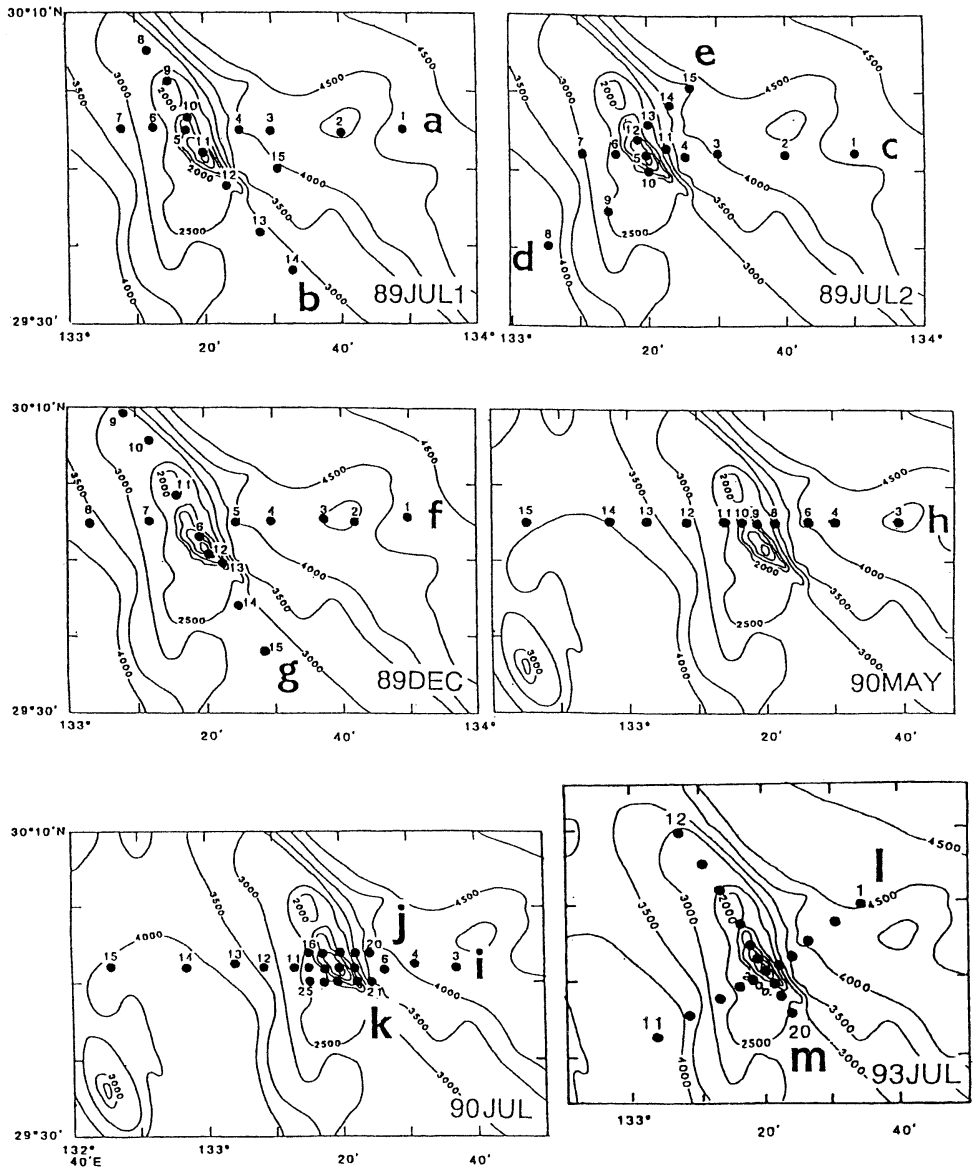

Fig. 3. CTD stations on each cruise. Letters, **a**–**m** identify sections and numbers identify stations.

observational periods. The CTD stations of the six cruises are shown in Fig. 3. KS–89JUL1, KS –89JUL2 and KS–89DEC sections were set NW-SE or NE-SW, parallel or normal to the longer axis of the seamount. In order to observe the background ocean conditions, a longer section was taken for all the observations. Unfortunately, because of CTD and ADCP trouble during KS－90JUL, Mi-com BT (T.S. MICOM-Bathythermograph 400A) by TSURUMI-SEIKI LTD. was used for the temperature observations. The accuracy of Mi-com BT is 0.05℃. Therefore, salinity data were not obtained by this cruise.

3. Results of observations

The vertical distributions of temperature along the sections **a**–**m** are shown in Figs. 4 and

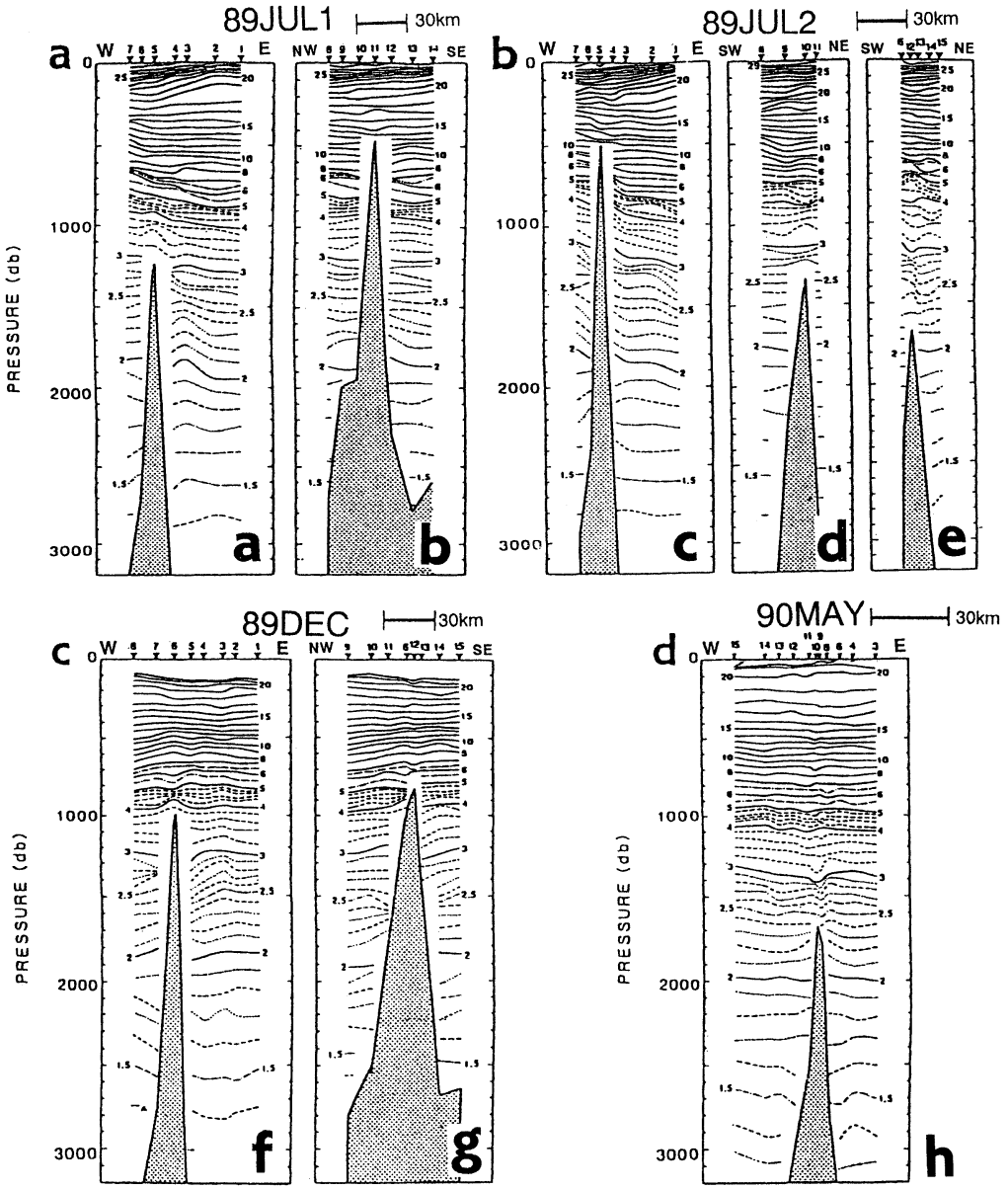

Fig. 4. Temperature sections (in ℃) along (a) sections **a** (left) and **b** (right), (b) sections **c** (left), **d** (middle) and **e**(right), (c) sections **f** (left) and **g** (right), and (d) section **h**(left). Observational section shown in Fig. 3 is shown in right bottom of each panel and observational stations are shown by closed triangles along the top.

5. Along section **a** of KS-89JUL1 (Fig. 4a left), upward shift of the isotherms is seen over the top of the seamount at depths of 850-1100 db. In layer deeper than the top of the seamount, isotherms between 1.7℃ and 2.5℃ show a vertically coherent upward shift in the eastern side of the seamount at depths of 1450-2200 db. In section **b** (Fig. 4a right), the uplift of isotherms over the top of the seamount is unclear: the 15 ℃ isotherm shows a weak downward shift, but the 17℃ isotherm shows an upward shift.

Along section **c** of KS-89JUL2 (Fig. 4b left),

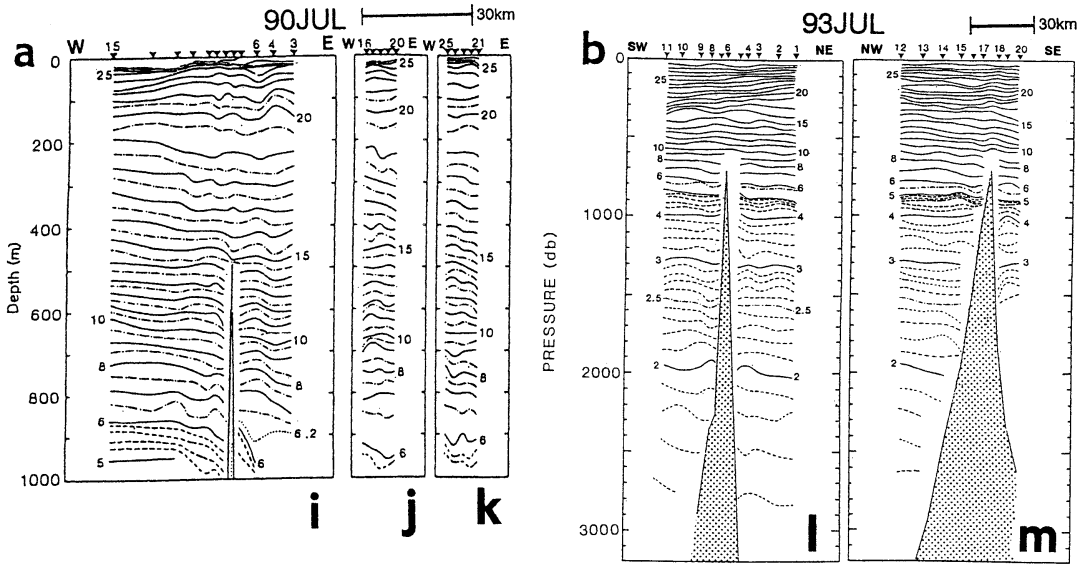

Fig. 5. Temperature sections (in ℃) along (a) sections **i** (left) and **j** (middle) and **k** (right), and (b) sections **l** (left) and **m** (right).

a clear uplift of isotherms is not seen over the seamount. Furthermore, the uplift of isotherms in the eastern side of the seamount observed in KS-89JUL1 (Fig. 4a left) is not observed. Since this observation was carried out in only one week after KS-89JUL1 (Fig. 4a), the temperature distribution over the top of the seamount is changed in a short time. However, the section **c** is located in south of section **a** (Fig. 1), spatial variation may be included. In water deeper than the top of the seamount, the 2-6 ℃ isotherms have a clear horizontal gradient over the eastern side slope. As the strong northward flow is observed in this observational period (Part II), the horizontal gradient of 2-6℃ isotherms are associated with the northward flow of small meander of the Kuroshio. Various vertical shifts of the isotherms are seen along section **d** and **e** (Fig. 4b middle and right).

In section **f** of KS-89DEC (Fig. 4c left), the formation of the mixed layer with a uniform temperature of 21℃ is seen in the surface layer, while seasonal thermocline is formed in the temperature fields in July (Figs. 4ab and 5ab). Isotherms are uplifted over the top of seamount at depths of 850-1000 db. Along section **g** (Fig. 4c right), gap of the depth of isotherm over the side slope between northwestern area and southeastern area is detected. Similar gap is seen in other sections. The gaps of isotherm have been also observed in other seamounts (e.g., FUKASAWA and NAGATA, 1978; SEKINE *et al.*, 1994).

In section **h** of KS-90MAY (Fig. 4d), coherent downward shift of the isotherms is found at depths of 1300-1700 db over the top of the seamount. This coherent downward shift is also seen in the salinity field (Fig. 6d). Some topographic effects of the seamount are suggested in these depths.

In section **i** of KS-90JUL (Fig. 5a left), isotherms are shifted downward at 400-500 db over the top of the seamount. However, the downward shift at 400-500 db is unclear along sections **j** and **k**, which suggests that the downward shift of the isotherms are confined to the top of the seamount. The depth gap of isotherms of 5℃ and 6℃ with different gradient over the side slope is very significant. In section **l** (Fig. 5b left), there is no clear vertical change in isotherms over the top of the seamount, while a relatively coherent weak upward shift of isotherms is detected along section **m**. Vertical shifts of the isotherms are seen at both sides of the seamount, however, their

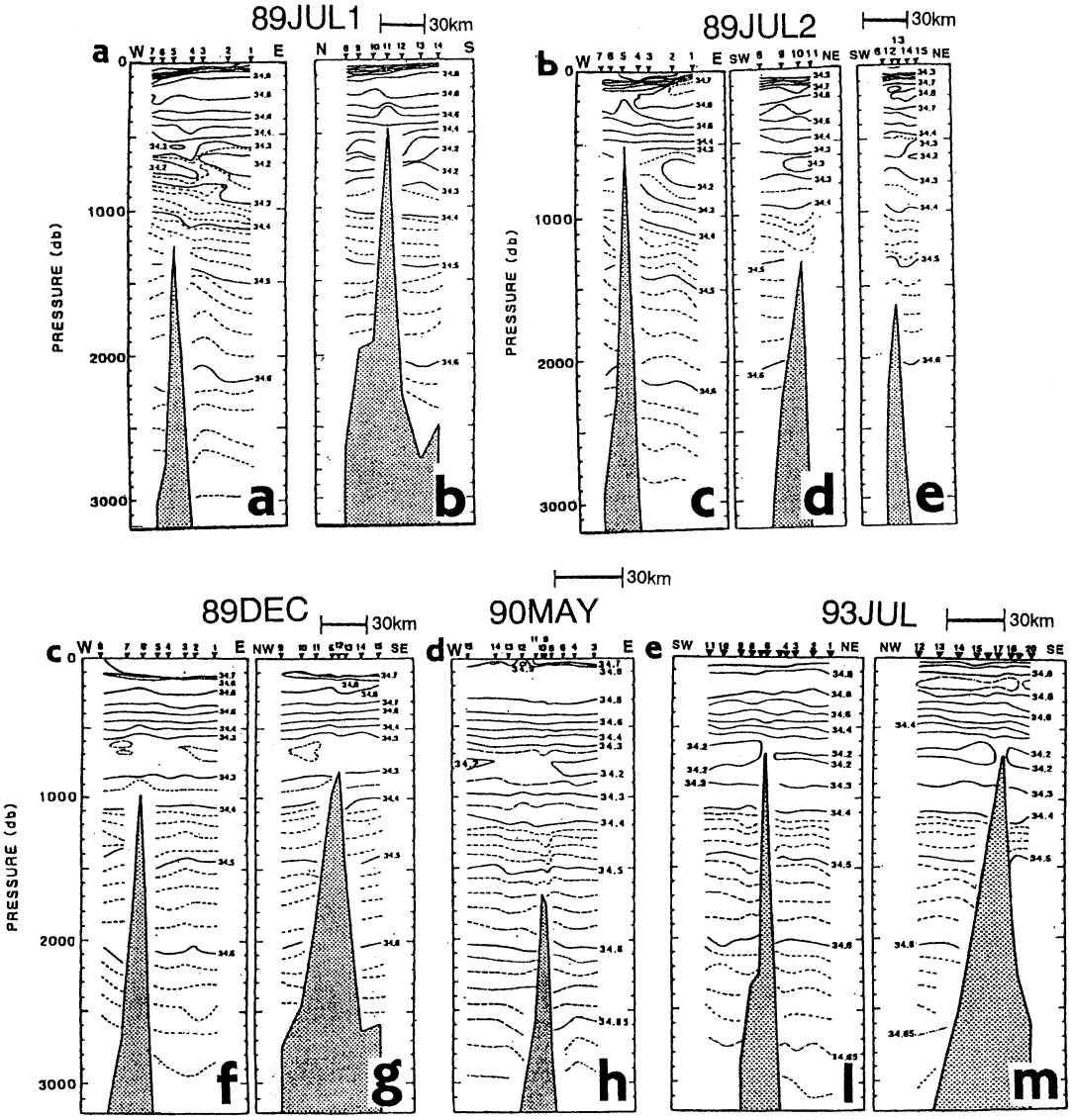

Fig. 6. Salinity sections (in psu) along (a) sections **a** (left) and **b** (right), (b) sections **c** (left), **d** (middle) and **e**(right), (c) sections **f** (left) and **g** (right), (d) section **h**(left) and (e) sections **l** (left) and **m**(right). Stations are shown by closed triangles along the top.

gradients are not confined to one specified direction to the bottom topography of the seamount.

The observed salinity fields are shown in Fig. 6. A salinity minimum water is commonly observed at depths 700–800 db. The salinity minimum corresponds to the North Pacific Intermediate Water (NPIW), which comes from east of the Izu Ridge to the Shikoku Basin (e.g., REID, 1965; YASUDA *et al.*, 1996; SEKINE *et al.*, 2000). In section **a** of KS-89JUL1, the salinity minimum layer (34.2 psu) is unclear over the top of seamount. Isohalines at depths of 1500–2200 db are shifted upward in the eastern side of the seamount, of which change are similar to those of the isotherms shown in Fig. 4a. The

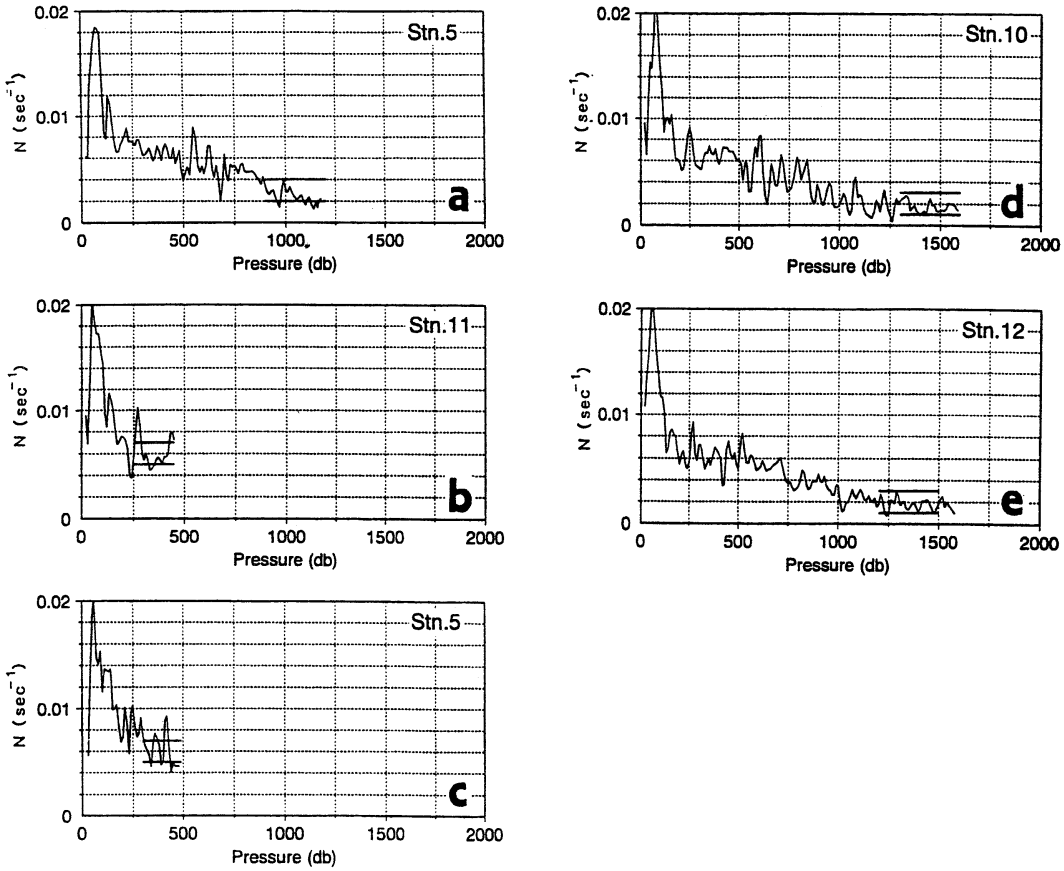

Fig. 7. Vertical distribution of Brunt-Väisälä frequency at the stations shown in the right top of each panel with shallowest depth in each observational line. (a) St. 5 of the observational line **a** in KS-89JUL1, (b) St. 11 of **b** in KS-89JUL1, (c) St. 5 of **c** in KS-89JUL2, (d) St. 10 of **d** in KS-89JUL2, (e) St. 12 of **e** in KS-89JUL2, (f) St. 6 of **f** in KS-89DEC, (g) St. 12 of **g** in KS-89DEC, (h) St. 9 of **h** in KS-90MAY, (i) St. 6 of **l** in KS-93JUL and (j) St. 17 of **m** in KS-93JUL.

similar change to temperature is also seen in Fig. 4b, in which changes associated with the approach of small meander of the Kuroshio is detected. Although the vertical shifts of the isohalines similar to those of isotherms are detected in most of other sections, the salimity minimum formed by NPIW is a characteristic phenomena and its distribuion gives new inflormation which is not seen in the temperature fields. Therefore, we focus on the change in the salinity minimum layer of NPIW over the seamount in the following.

It should be noted that less saline water less than 34.25 psu does not exist just above the top of the seamount (Fig. 6 bcde). In particular, clear salinity minimum water less than 34.2 psu is detected in the western and eastern side of the seamount (Fig. 6e), but such a less saline water is not seen over the top the seamount. These common features suggest that the unclear salinity minimum over the top of the seamount is caused by enhanced vertical mixing over the top of the seamount by the internal wave generated by the seamount and/or by the topographic effect of the seamount, which forces a less salinity water to flow along isopleths of depth around the top of the seamount. Unclear less saline water (NPIW) over the top of the seamount is also observed over the Daini Kinan Kaizan (SEKINE and HAYASHI, 1992) and Tosa-Bae (SEKINE, *et al.*, 1994).

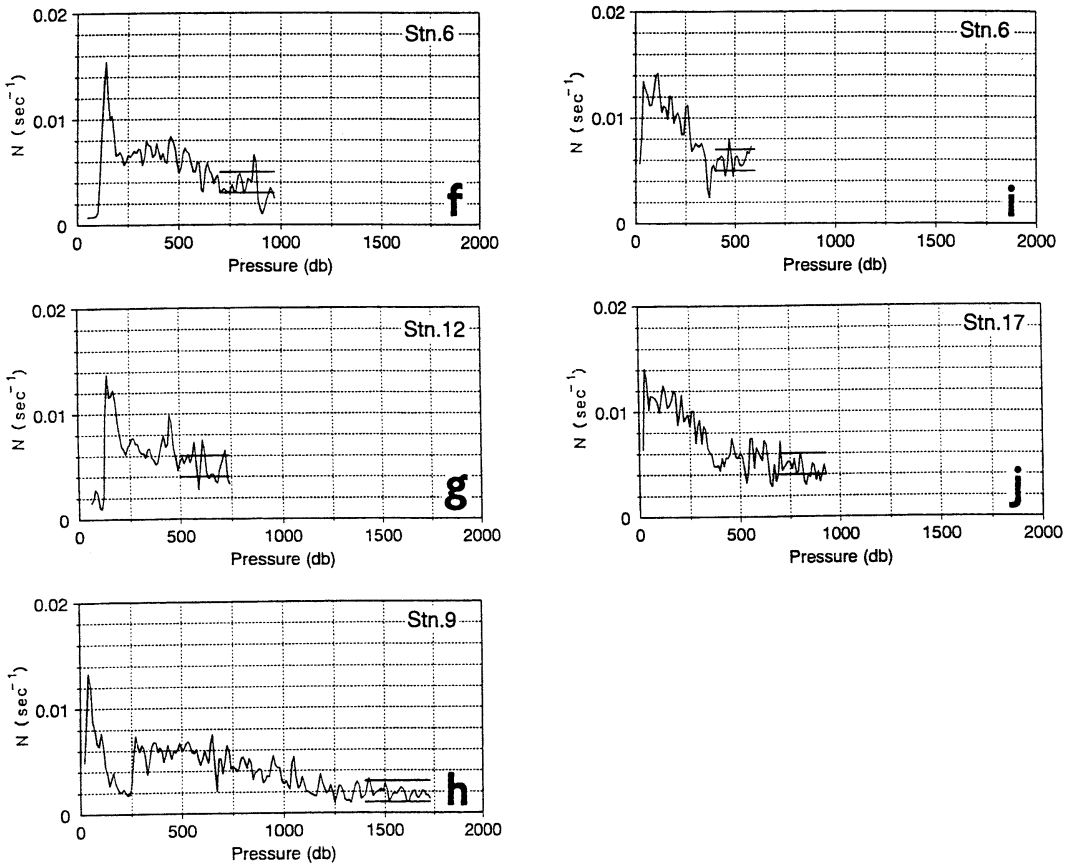

Fig. 7. (f) St. 6 of **f** in KS-89DEC, (g) St. 12 of **g** in KS-89DEC, (h) St. 9 of **h** in KS-90MAY, (i) St. 6 of **l** in KS-93JUL and (j) St. 17 of **m** in KS-93JUL.

4. Topographic effect of the Komahashi Daini Kaizan

If we assume constant Brunt-Väisälä frequency (N) and "bell-shaped" seamount with a height of $h_0/(1+(x/L)^2)$, where h_0 is a peak height and x the horizontal distance from the peak of the seamount and L half of the representative horizontal scale of the seamount, the topographic effect of a seamount is well estimated by the Rossby height (fL/N), where f is the Coriolis parameter (e.g., GILL, 1982). Although these conditions are not exactly fulfilled in the present case, we can estimated the possible range of Rossby height by considering the possible maximum and minimum value of N and L. Vertical distribution of the observed N over the top of the seamount is shown in Fig. 7, in which approximated range of N used in the estimation is also shown. It is shown from Fig. 7 that N is large in the seasonal thermocline layer near the sea surface and N becomes small below the permanent thermocline layer where we set the variable range of N.

Assuming the maximum and minimum L as in Table 2, the estimated Rossby height (RH) and the height of the observed baroclinic Taylor column (HT) are shown in Fig. 8. Here, only coherent or evanescent vertical changes in the observed temperature from the bottom topographies are considered in the evaluation of observed HT, while those of which maximum vertical displacement is separating from the bottom topographies of the seamount are neglected. It is shown from Fig. 8 that RH varies significantly, depending on the estimated L and N. Although positive correlation is detec-

Table 2. Estimated Rossby height (RH = fL/N)

Cruise name	Observational line	N (sec^{-1})	L(km)		RH(Rossby height)(m)	
			Mimimum	Maximum	Minimum	Maximum
KS-89JUL1	**a**	2×10^{-3}	2.7	4.5	97	162
		3×10^{-3}			65	108
		4×10^{-3}			49	81
	b	5×10^{-3}	2.7	5.5	39	79
		6×10^{-3}			32	66
		7×10^{-3}			28	57
KS-89JUL2	**c**	5×10^{-3}	2.0	3.8	29	55
		6×10^{-3}			24	46
		7×10^{-3}			21	39
	d	1×10^{-3}	3.9	7.5	280	540
		2×10^{-3}			140	270
		3×10^{-3}			94	180
	e	1×10^{-3}	3.0	6.0	216	432
		2×10^{-3}			108	216
		3×10^{-3}			72	144
KS-89DEC	**f**	3×10^{-3}	2.3	4.5	55	108
		4×10^{-3}			41	81
		5×10^{-3}			33	65
	g	4×10^{-3}	6.0	11.3	108	203
		5×10^{-3}			87	163
		6×10^{-3}			72	136
KS-90MAY	**h**	1×10^{-3}	2.7	3.8	194	274
		2×10^{-3}			97	137
		3×10^{-3}			65	91
KS-93JUl	**l**	5×10^{-3}	2.5	3.5	36	50
		6×10^{-3}			30	42
		7×10^{-3}			26	36
	m	4×10^{-3}	4.0	7.0	72	126
		5×10^{-3}			58	101
		6×10^{-3}			48	84

ted, they do not exceed the 95% confidence limit ($\gamma = 0.63$). It is resulted from Table 2 that almost of eatimated RH is smaller than the depth of the peak of the seamount (289 m), in which only two maximums ranges exceed the depth of seamount. As for HT, it is clear from Figs. 4, 5 and 6 that the baroclinic Taylor column does not reach to the upper layer. These two results demonstrate that the topographic effect of the Komahashi Daini Kaizan does not reach to the surface.

5. Summary and discussion

The hydrographic observations around Komahashi Daini Kaizan south of Japan were made by the Training Vessel "Seisui-maru" of Mie University for six times from 1989 to 1993. Main results of the observations are summarized as follows.

(1) A salinity minimum layer of NPIW is observed at depths 700–800 db in all the observations. Over the top of the seamount, the salinity minimum layer is relatively unclear in comparison with that in the surrounding area. It is suggested that salinity minimum water less than 34.2 psu is vertically mixed relatively well by the internal wave over the top of the seamount and/or is forced to flow along

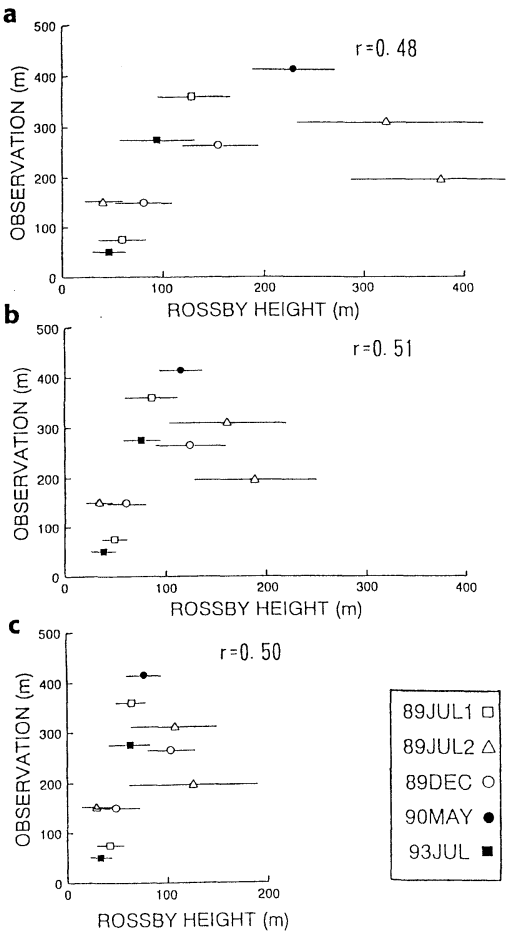

Fig. 8. Correlation between the estimated Rossby height (fL/N) evaluated from the observed N and the observed baroclinic Taylor column estimated from the vertical changes of isotherms and isohalines. (a) Case of minimum possible Brunt-Väisälä frequency (N), (b) midrange N and (c) maximum possible N. Horizontal bars show the possible ranges of Rossby height depending on the representative horizontal scale of the Komahashi Daini Kaizan (L).

isopleth of depth of the seamount.

(2) In July 1989, the siginificant change in the temperature and salinity fields are observed during only one week. This is due to the approach of small meander of the Kuroshio generated in southeast of Kyushu. Although the spatial change is included, short period time change is shown to be possible in the vicinity of Komahashi Daini Kaizan.

(3) Although the observed Rossby height (fL/N) RH varies significantly depending on the estimated L and the observed N, it is shown that most of eatimated RH is smaller than the depth of the peak of the seamount (289 m). The observed height of baroclinic baroclinic Taylor column (HT) estimated from isotherm and isohaline does not reach to the upper layer. These two facts result that the topographic effect of the Komahashi Daini Kaizan does not reach to the surface.

As is mentioned in (2), significant differences of temperature and salinity fields are observed between KS-89JUL1 and KS-89JUL2 only one week apart. These observational results strongly suggest that more frequent observations are needed to see the detailed oceanic conditions over and around this seamount. It should be also noted that we have no clarified way to filter the contribution of internal wave to the vertical change in the isotherms and isohalines. This problem is more serious in the estimation of the geostrophic flow. Namely, all the vertical change in isotherms are not associated with the geostrophic balance and the contribution of internal waves are not negligible. It is pointed out that some correction which possibly excludes the internal wave is needed for the estimation of geostrophic flow.

Although it is suggested that the topographic effect of the Komahashi Daini Kaizan does not fully reach to the surface (3), the topographic effect on the distribution of the salinity maximum layer denoted in (1) indicates the topographic effect of the seamount reaches to this depth, if a salinity minimum water is forced to flow along isopleth of depth of the seamount. However, if the salinity minimum water is vertically mixed relatively well by the internal wave generated over the top of the seamount, the topographic effect is made through the internal wave, which is different from the effect of the baroclinic Taylor Column. Unfortunately, we can not determine which is more importnant over this seamount. To see this more clearly, non-geostrophic topographic effect of the seamount such as the generation of internal wave should be observed in the future study.

Acknowledgments

I am indebted to Captain Isamu ISHIKURA, the officers and the crews of the Training Vessel "Seisui-maru" of Mie University for their skillful assistance during the six cruises. The author would like to thank Dr. H. SOLOMON for his critical reading of the manuscript with valuable comments. Thanks are also extended to many students and post graduate students of Mie University, Messrs. Yuichi SATO now at Tohoku Center of Japan Weather Association, Toshiaki KOMATSU now at Kokusai Kogyo Co., LTD., Motoya NAKAGAWA now at Mie Center of Fuyo Ocean Development and Engineering, Haruki OHWAKI now at PASCO Cooperation, Atsushi FUKUTOMI now at SHOKOZAN Mining Co., Ltd. for their help in observation and assistance in drawing some figures. This work was partly supported by a Grant-in-Aid for Scientific Research on Priority Areas from the Ministry of Education (Grant No. 03248109).

References

FUKASAWA, M. and Y. NAGATA (1978): Detailed oceanic structure in the vicinity of the Shoal Kokusho-sone. J. Oceanogr. Soc. Japan, **34**, 41–49.

FUKASAWA, M. and Y. NAGATA (1980): Cold water areas in the vicinity of the Shoal Kokusho-sone. J. Oceanogr. Soc. Japan, **36**, 141–150.

FUKASAWA, M. (1983): On the distribution of isothermal layers in the vicinity of the Shoal Kokusho-sone. J. Oceanogr. Soc. Japan, **39**, 15–21.

GILL, A. E. (1982): Atmosphere-Ocean dynamics. Academic Press, New York, London, 662pp.

KONAGA, S. and K. NISHIYAMA (1978): Behavior of a detached eddy "Harukaze" around the seamount of Daiiti- and Daini-Kinan Kaizan. Pap. Meteor. Geophys., **29**, 115–156 (in Japanese with English abstract).

KONAGA, S. K. NISHIYAMA and H. ISHIZAKI (1980): Some effects of seamounts on the Kuroshio path. Proc. 4th CSK Symp. 1979, 218–231.

RIED, J. L. (1965): Intermediate Waters of the Pacific Ocean. John Hopkins Press, 85 pp.

SEKINE, Y. and Y. TOBA (1981): Velocity variation of the Kuroshio during the formation of small meander south of Kyushu. J. Oceanogr. Soc. Japan, **37**, 87–93.

SEKINE, Y. and Y. MATSUDA (1987a): Hydrographic structure around the Tosa- Bae, the bump off Shikoku south of Japan, in November 1985. La mer, **25**, 137–146 (in Japanese with English abstract).

SEKINE, Y. and Y. MATSUDA (1987b): Observation on surface mixed layer around the Tosa-Bae, the Bump off Shikoku south of Japan in November 1985. Umi to Sora, **63**, 1–14 (in Japanese with English abstract).

SEKINE, Y. and T. HAYASHI (1992): Oceanic structure in the vicinity of a seamount, the Daini Kinan Kaizan, south of Japan. La mer, **30**, 17–26.

SEKINE, Y., H. OHWAKI and M. NAKAGAWA (1994): Observation of oceanic structure around Tosa-Bae southeast of Shikoku. J. Oceanogr., **50**, 543–558.

SEKINE, Y., S. WATANABE and F. YAMADA (2000): Topographic effect of Izu Ridge on the distribution of the North Pacific intermediate water south of Japan. J. Oceanogr., **56**, 429–438.

SEKINE, Y. (2001): Oceanic structures in the Vicinity of Komahashi Daini Kaizan, a Seamount in the Kyushu-Palau Ridge. Part II Velocity Fields. La mer, **39**, 107–112.

SHOJI, D. (1972): Time variation of the Kuroshio south of Japan. In: Kuroshio - Its Physical aspects of the Japan Current, STOMMEL, H. and K. YOSHIDA, (eds.) , Univ. Washington Press., Seattle, 217–234.

SOLOMON, H. (1978): Occurrence of small "trigger" meander in the Kuroshio off southern Kyushu. J. Oceanogr. Soc. Japan., **34**, 81–84.

TAFT, B. (1972): Characteristics of the flow of the Kuroshio south of Japan. *In*: Kuroshio- Physical aspects of the Japan Current, STOMMEL, H. and K. YOSHIDA, (eds.) Univ. Washington Press., Seattle, 165–214.

YASUDA, I., K. OKUDA and Y. SHIMIZU (1996): Distribution and modefication of North Pacific Intermediate Water in the Kuroshio-Oyashio interfrontal zone. J. Phys. Oceanogr., **26**, 448–465.

Received on August 29, 2000
Accepted on May 1, 2001

La mer 39 : 107–112, 2001
Société franco-japonaise d'océanographie, Tokyo

Oceanic structures in the vicinity of Komahashi Daini Kaizan, a seamount in the Kyushu-Palau Ridge Part II. Velocity Fields

Yoshihiko SEKINE*

Abstract : Hydrographic observations in the vicinity of a seamount, Komahashi Daini Kaizan, located in the northwestern part of the Philippine Basin south of Japan, were carried out six times from 1989 to 1993. As the results on the temperature and salinity fields obtained by these cruises have been reported in Part I, results of velocity fields by ADCP are presented in this paper. Most of the observed velocity by ADCP goes over the seamount, Komahashi Daini Kaizan and a tendency to flow along the isopleth of the depth of the seamount is shown to be weak, which indicates the topographic effect of the seamount does not reach to the deepest level of ADCP data of 150 m–200 m. This result agrees with Part I which shows that the observed Rossby height (fL/N) and the observed baroclinic Taylor column estimated from the change in isotherm and isohaline are smaller than the representative depth of the seamount. In July, 1989, vertically coherent large northward velocity was observed in association with the formation of small meander path of the Kuroshio southeast of Kyushu. The attainment of geostrophic balance is checked by the correlation between the observed vertical difference of geostrophic flow and that of ADCP velocity. Although positive correlation is detected between the two velocity differences, they do not show clear linear relation. This suggests that non-geostrophic flow component is prominent in the vicinity of this seamount.

Key words : *Komahashi Daini Kaizan, Kyushu-Palau Ridge, topographic effect, sea mount*

1. Introduction

The interaction of ocean currents with seamounts has been of interest to the oceanic community (e.g., HOGG, 1980; RODEN, 1987). Generation of internal waves, trapping and/or generation of eddies and uplift of deeper layer water are possible by the topographic effects of a seamount. The effects of a seamount generally depend on the vertical structure of the Taylor column formed over the seamount (e.g., HOGG, 1973; JOHNSON, 1977). If the water has a homogeneous density and the nonlinear effect is relatively small, a barotropic Taylor column with vertically coherent flow is formed and the topographic effect of the seamount extends to the surface layer. If these two conditions are not satisfied, the Taylor column has a tendency to be restricted to a deeper level below the Rossby height fL/N (e.g., GILL, 1982), where f is the Coriolis parameter, L the half of the representative horizontal scale of seamount with a depth of $h_0/(1+(x/L)^2)$, where h_0 is a height of the peak of the seamount from ocean basin and x a horizontal distance from the peak and N the Brunt-Väisälä frequency assumed constant.

Furthermore, the topographic effect of an elliptic seamount placed at various angles to a uniform barotropic flow was examined by JOHNSON (1982) and the planetary β effect on the topographic effect of a seamount was examined by MCCARTNEY (1975) and VERRON and LE PROVOST (1985). The detailed time change of the topographic effect was studied by HUPPERT and BRYAN (1975).

Although there have been various theoretical studies, the observations on the topographic effect of the seamount have not been fully carried out. Because oceanic conditions are different for each seamount, specified

* Institute of Oceanography, Faculty of Bioresources, Mie University, 1515 Kamihama, Tsu, Mie, 514–8507 Japan

observations on the topographic effect of seamount are needed for each seamount. In part I of this study (SEKINE, 2001), the observed oceanic conditions over the seamount "Komahashi Daini Kaizan" in the Kyushu-Palau Ridge in the Philippine Basin was reported with reference to temperature and salinity fields. In the present paper, the observed velocity fields in the vicinity of Komahashi Daini Kaizan is reported as a Part II of this study.

2. Observations

Observations have been carried out using the Training Vessel "Seisui-maru" of Mie University from 1989 to 1993. An acoustic doppler current profiler (ADCP) was used to observe the horizontal velocity along CTD observational lines, of which details have been mentioned in Part I. The ADCP data averaged every ten minites with the accuacy of 5 cm sec^{-1} were corrected by use of GPS data and loran C data. Only the ADCP velocity observed during constant ship speed are analyzed in the present study.

3. Results of observations

Velocity fields observed by ADCP is shown in Fig. 1. In KS-89JUL1 (Fig. 1a) observed from 14 to 16 in July 1989, southward flow dominates at 50 m, but northward flow dominates at 100 m and 150 m. Coherent flows are found at 100 m and 150 m, except for the western area of the seamount.

Vertically coherent strong northeastward flow is observed in KS-89JUL2 (Fig. 2b) observed from 22 to 24 in July 1989. As this observation is made about one week after KS-89JUL1 (Fig. 1a), very significant change in the flow pattern is detected. A small meander of the Kuroshio off Kyushu is formed in this observational period (Part I) and the strong northeastward flow is associated with the small meander of the Kuroshio. It should be noticed that the large meander of the Kuroshio is formed by the eastward shift of the small meander southeast of Kyushu and its abrupt amplification in south of Kii Peninsula (SHOJI, 1972; SOLOMON, 1978; SEKINE and TOBA, 1981a). In particular, SEKINE and TOBA (1981b) pointed out by the numerical experiments that the small meander can be generated by the stretching of the water column over the continental slope, when the current velocity of the Kuroshio is abruptly increased. Similar results were obtained by ENDOH and HIBIYA (2000) by use of a flat bottom model, in which small meander is formed by the coastal topographic effect of Kyushu during the period of increase in the Kuroshio velocity.

During KS-89DEC (Fig. 1c), vertically coherent northwestward flow was seen east of the seamount. Together with the southwestward flow west of the seamount, existence of cyclonic circulation is suggested over and around the seamount. Vertically coherent flow is detected in KS-90MAY (Fig. 1d). In KS-93JUL (Fig. 1e), coherent eastward flow is observed in the northern region at depths 50 m and 100 m. Although the flow is vertically coherent down to 200 m in the east, clear eastward flow at 200 m is not found in the north.

If the topographic effect of the seamount is prominent in the upper layer, there is a tendency that the flow over the seamount has a tendency to flow along contours of ambient potential vorticity f/h, which is well approximated by the contours of h (isopleth of depth). Here, as the topographic effect is relatively prominent in the deeper layer, we notice the ADCP velocity at the deepest layer near the seamount.

In KS-JUL1 (Fig. 1a), as the northward flow goes over the top of the seamount, the velocity pattern shows no tendency to flow along isopleth of depth. In KS-89JUL2 (Fig. 1b), the small meander flow goes over the seamount. Because the inertial effect of the small meander is so large (SEKINE and TOBA, 1981ab; ENDOH and HIBIYA, 2000), and because horizontal scale of the small meander is much larger than the scale of the seamount, it is suggested that the small meander can go eastward over the seamount.

The southwestward flows goes over the seamount in KS-89DEC (Fig. 1c) and KS-90MAY (Fig. 1d), while the northeastward flow also goes over the seamount in KS-93JUL (Fig. 1e). On the whole, most of the flow goes over the top of seamount and tendency to flow along the isopleth of the depth of the seamount

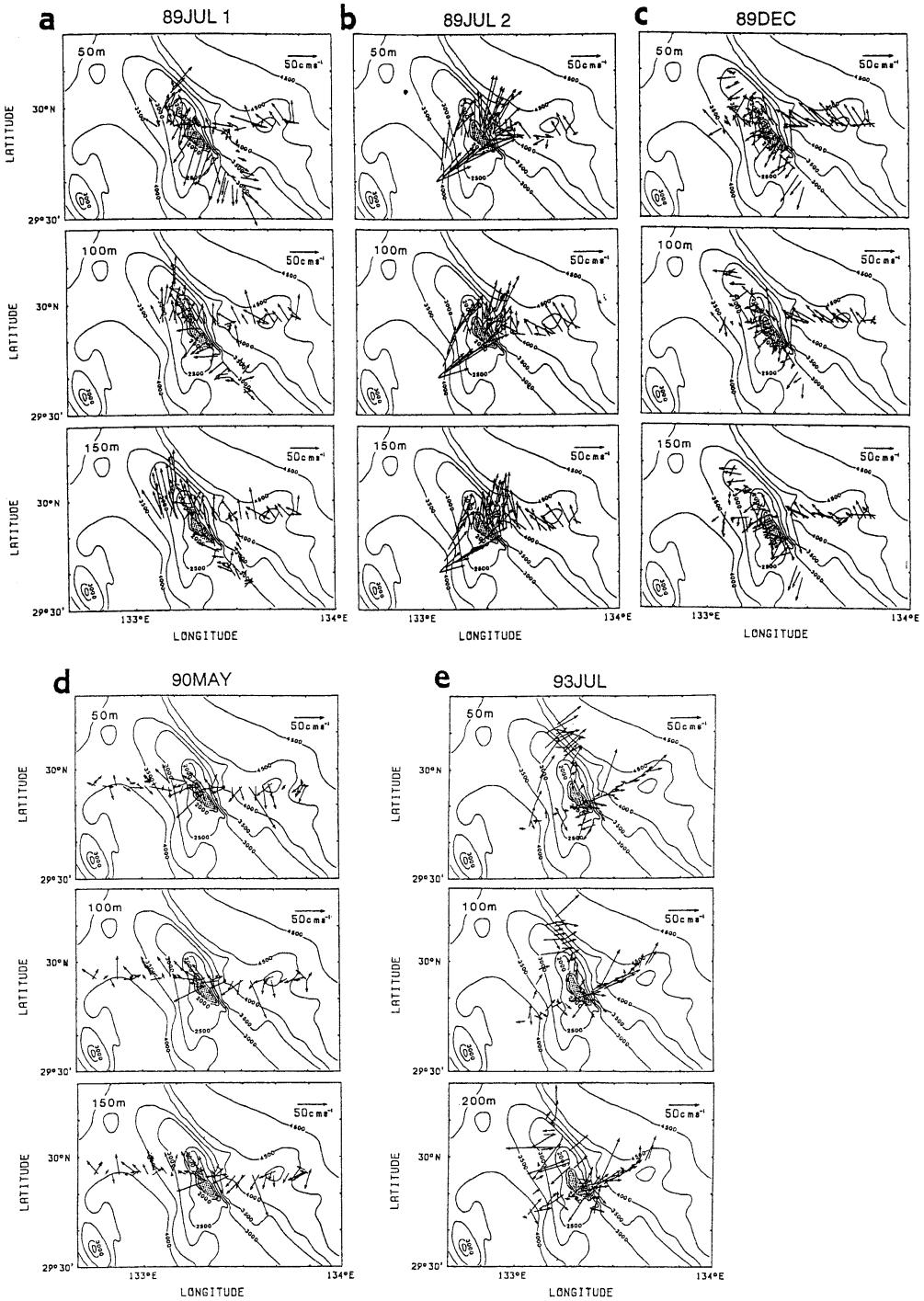

Fig. 1. Horizontal velocity observed by ADCP during (a) KS-89JUL1, (b) KS-89JUL2, (c) KS-89DEC, (d)KS-90MAY and (e) KS-93JUL. Isopleths of depths (in meters) are also shown in top left of each panel. Region shallower than 1500 m is stippled.

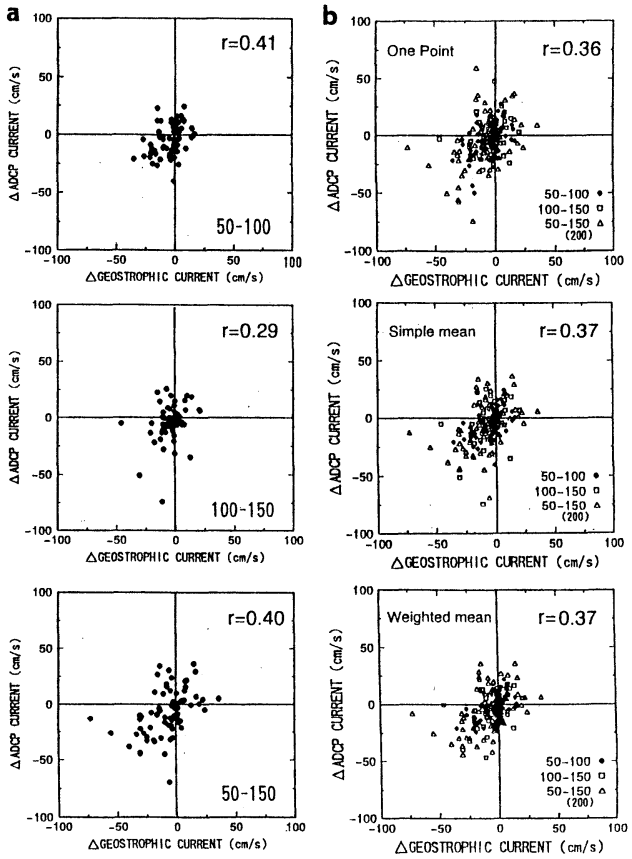

Fig. 2. (a) Correlation between the vertical differences of geostrophic velocity and of observed ADCP velocity. The vertical difference of ADCP is estimated as mean of all the ADCP velocities observed between two neighboring CTD stations. Two levels (in depth) to estimate the velocity difference are shown right bottom and the correlation coefficient (r) is shown in the upper right of each panel. (b) Correlation between the vertical geostrophic flow difference and observed ADCP velocity difference at 50 ~ 150 m. ADCP velocity is estimetd as one ADCP data nearest to the middle point of the two neighboring CTD stations (top) and same as in (a) (middle) and as the weighted mean of all the ADCP velocity, in which the weight is inversely proportional to the distance of the ADCP station from the middle point between two CTD stations (bottom).

is shown to be weak, which indicates the topographic effect of the seamount does not reach to the deepest level of ADCP data of 150 m–200 m. This result agrees with Part I, in which the observed Rossby height (fL/N) and the observed baroclinic Taylor column estimated from the change in isotherm and isohaline are smaller than the representative depth of the Komahasi Daini Kaizan, which indicates that the topographic effect of the Komahashi Daini Kaizan does not reach to the surface.

In order to see the attainment of the geostrophic balance over the seamount, correlation between the vertical difference of geostrophic flow and that of velocity observed by ADCP is shown in Fig. 2. Here, we should notice that the vertical difference of the geostrophic flow does not depend on the selection of the reference level (Fig. 3). Namely, the constant barotropic flow due to the unknown surface pressure gradient equally acts on the internal layer, it is eliminated by the difference of two internal levels. Here, ADCP velocity is estimated as the simple mean of all ADCP

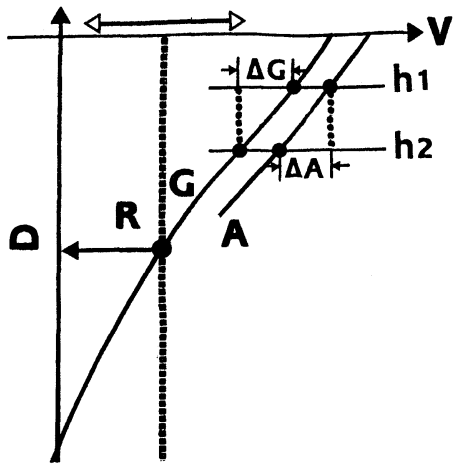

Fig. 3. Schematic representation of the analysis to see the attainment of the geostrophic flow balance. Horizontal (vertical) axis shows the velocity (depth). Because only the vertical Geostrophic flow profile (G) is obtained by the geostrophic flow estimation, actual geostrophic velocity shifts parallel to horizontal axis illustrated by open arrows, which depends on the adoption of the reference level shown by R. This effect can be negected, if we consider the vertical geostrophic flow difference at two different depth, H1 and H2. So attainment of the geostrophic flow balance is examined by comparing the vertical velocity difference of the geostrophic flow and that of ADCP velocity (A).

velocity data between two neighboring CTD stations. It is shown from Fig. 2a that although positive correlation exceeds the confidence limit of 95 % with the correlation coefficient ($\gamma = 0.24$), two velocity differences do not shows clear linear relationship.

Because there are several observed ADCP velocities between two neighboring CTD stations, other two ADCP velocities are estimated : the first is one ADCP data nearest to the middle point of the two neighboring CTD stations and the second is estimated as the weighted mean of all the ADCP velocity between two neighboring CTD stations, in which the weight is inversely proportional to the distance of the ADCP station from the middle point between two CTD stations. It is shown from Fig. 2b that they show no significant systematic difference and the correlation coefficient is almost equal. This means that there exists a non-geostrophic flow component such as the tidal current, the wind-drift flow and/or the Ekman flow, which agrees with the case of the seamount Daini Kinan Kaizan (SEKINE and HAYASHI, 1992) and Tosa-bae (SEKINE *et al.*, 1994).

5. Summary and discussion

The hydrographic observations around Komahashi Daini Kaizan south of Japan were made by the Training Vessel "Seisui-maru" of Mie University six times from 1989 to 1993. As a Part II of this study, observed velocity by use of ADCP is reported in the present paper. Main results are summarized as follows.

(1) Almost of the flow goes over the seamount and tendency to flow along the isopleth of the depth of the seamount is shown to be weak (Fig. 1), which indicates the topographic effect of the seamount does not reach to the deepest level of ADCP data of 150 m–200 m. This result agrees with Part I in which the observed Rossby height (fL/N) and the observed baroclinic Taylor column estimated from the change in isotherm and isohaline are shown to be smaller than the representative depth of the seamount.

(2) In KS-89JUL2 (Fig. 1b), vertically coherent large northward velocity was observed in association with the formation of small meander path of the Kuroshio southeast of Kyushu. As this observation is made about one week after KS-89JUL1 (Fig. 1a), significant change in the velocity fields is detected. The approach of the Kuroshio has a large influence on the oceanic condition of this seamount.

(3) In order to see the attainment of geostrophic balance, correlation between the vertical difference of geostrophic flow and that of ADCP velocity has been examined. Although significant positive correlation is obtained between the two velocity differences, they do not show clear linear relation. Non-geostrophic flow component is not negligible in the vicinity of this seamount in the upper layer shallower than 150–200 m.

Non-geostrophic flow component is important in the upper layer, which is mentioned in (3). In relation to this, it should be noted that ADCP velocity is often used as a reference

velocity of the geostrophic flow estimation. However, there is a possibility that the geostrophic flow balance is not established in the ADCP velocity (3). As the check of the attainment of the geostrophic balance (Fig. 3) is easily carried out, such a check is needed if ADCP velocity is used as a reference level velocity. In relation to this, it should be also noted that we have no clear method to filter the contribution of the vertical change in the isotherms and isohalines which has no relationship of the geostrophic flow balance such as internal wave. Namely, all the vertical changes in isotherms and isohaline are not associated with the geostrophic flow balance and their contribution on the pressure gradient is included in the geostrophic flow estimation. Some correlation method which excludes the internal pressure gradient by non-geostrophic temperature and salinity variations is needed for the exact estimation of geostrophic flow.

Acknowledgments

The authors would like to thank Dr. H. SOLOMON for his critical reading of the manuscript. We are indebted to Captain Isamu ISHIKURA, the officers and the crews of the Training Vessel Seisui-maru of Mie University for their skillful assistance during the cruises. Thanks are also extended to many students and post graduate students of the Faculty of Bioresources of Mie University, Messrs. Yuichi SATO, Toshiaki KOMATSU, Motoya NAKAGAWA, Haruki OHWAKI and Atsushi FUKUTOMI (for their present affiliation, see Part I) for their help in observation. This work was partly supported by a Grant-in-Aid for Scientific Research on Priority Areas from the Ministry of Education (Grant No. 03248109).

References

ENDOH, T. and T. HIBIYA (2000): Numerical study of the generation and propagation of trigger meander of the Kuroshio south of Japan. J. Oceanogr., **56**, 409–418.

GILL, A. E. (1982): Atmosphere–Ocean dynamics. Academic Press, New York, London, 662pp.

HOGG, N. G.(1973): On the stratified Taylor column. J. Fluid Mech., **58**, 517–537.

HOGG, N. G.(1980): Effects of bottom topography on ocean currents. Orographic Effects in Planetary Flows, GARP Publication Ser., No.23, 167–205.

HUPPERT, H. E. and K. BRYAN (1976): Topographically generated eddies. Deep-Sea Res., **23**, 655–679.

JOHNSON, E. R. (1977): Stratified Taylor Column on a beta-plane. Geophys. Astrophys. Fluid Dyn., **9**, 159–177.

JOHNSON, E. R. (1982): Quasigeostrophic flow over isolated elongated topography. Deep-Sea Res., **29**, 1085–1097.

MCCARTNEY, M. S. (1975): Inertial Taylor column on a beta plane. J. Fluid Mech., **68**, 71–95.

RODEN, G. I. (1987): Effects of seamounts and seamount chains on oceanic circulation and thermocline structure. Seamounts, Islands and Atolls. KEATING, B. ed., Geophys. Monogr. American Geophysical Union, **43**, 335–354.

SEKINE, Y. and Y. TOBA (1981a): Velocity variation of the Kuroshio during the formation of small meander south of Kyushu. J. Oceanogr. Soc. Japan, **37**, 87–93.

SEKINE, Y. and Y. TOBA (1981b): A numerical experiment of the generation of the small meander of the Kuroshio off southeastern Kyushu. J. Oceanogr. Soc. Japan, **37**, 234–242.

SEKINE, Y. and T. HAYASHI (1992): Oceanic structure in the vicinity of a seamount, the Daini Kinan Kaizan, south of Japan. La mer, **30**, 17–26.

SEKINE, Y., H. OHWAKI and M. NAKAGAWA (1994): Observation of oceanic structure around Tosa-Bae southeast of Shikoku. J. Oceanogr., **50**, 543–558.

SEKINE, Y. (2001): Oceanic structures in the Vicinity of Komahashi Daini Kaizan, a seamount in the Kyushu Palau Ridge. Part I Temperature and salinity fields. La mer, **39**, 95–106.

SHOJI, D. (1972): Time variation of the Kuroshio south of Japan. In: Kuroshio-Physical aspects of the Japan Current, STOMMEL H. and K. YOSHIDA, Eds., Univ. Washington Press, Seattle, 517pp.

SOLOMON, H. (1978): Occurrence of small "trigger" meander in the Kuroshio off southern Kyushu. J. Oceanogr. Soc. Japan, **34**, 81–84.

VERRON, J. and C. Le PROVOST. (1985): A numerical study of quasi-geostrophic flow over isolated topography. J. Fluid Mech., **154**, 231–252.

Received on August 29, 2000
Accepted on May 1, 2001

La mer 39 : 113, 2001
Société franco-japonaise d'océanographie, Tokyo

資　料

第39巻第2号掲載欧文論文要旨

Ivonne M. Radjawane* ・松山優治* ・北出裕二郎* ・鈴木　亨 ：東京湾の密度流に関する数値実験**

河川から流入する淡水により形成される東京湾の密度流について，3次元レベルモデルを用いて調べた。数値実験は，成層した湾内部に河川から放出された低密度水がつくる流れと，密度分布に焦点を合わせて行われた。低密度水は河口から最大3-5 cm/sのスピードを持ち，コリオリの力を受けて非対称的な形状をしながら表層を拡がっていく。放出された低密度水は河口を中心にして時計回りの循環を形成する。この表層水のすぐ下の中層に，河口に向かう非常に弱い流れが形成される。河口に向かう流れは，表層を沖に向かう流れによる連行として引き起こされたものと考えられる。(*東京水産大学海洋環境学科　〒108-8477　東京都港区港南4-5-7，**日本水路協会海洋情報研究センター　〒104-0061　東京都中央区銀座7-15-4　三島ビル5F)

Suhendar I. Sachoemar* ・柳　哲雄 ：ジャワ北岸海洋の水質の季節変動**

ジャワ島北岸海域の水質の季節変動の実態と，それを決める要因を明らかにするために，1979-81年に得られた観測データの解析を行った。水温，塩分，密度は1月(北西モンスーン：雨季)に低く，9月(南東モンスーン：乾季)に高い。栄養塩濃度は河川からの付加と卓越沿岸流の影響を受け，リン酸は中央部で1月に，西部では9月に高い。珪酸と硝酸は東部で1月に，西部で9月に高い。レッドフィールド比は全域で16より小さく，硝酸が基礎生産の律速栄養塩になっている。クロロフィルa濃度は，中央部と西部で1月に高いが，東部では9月に高い。(*九州大学大学院総合理工学府，**九州大学応用力学研究所　〒816-8580　福岡県春日市春日公園6-1)

関根義彦* ：九州パラウ海嶺にある駒橋第二海山近辺の海洋構造　第1部　水温および塩分分布

九州パラウ海嶺中にある海山「駒橋第二海山」の近隣で，1989年から1993にわたり，6回のCTDとADCPによる海洋観測を行った。本論では，これらの観測の論文の第一部として水温と塩分分布の結果を示した。等温線と等塩分線の上下変化が数多く見られ，ほぼ全観測で34.2 psu以下の低塩分水が駒橋第二海山の直上および斜面上では観測されず，海山を離れた海域で観測された。これについては塩分極小層を成す北太平洋中層が，海山上で内部波による大きな鉛直混合を受ける，あるいは，海山の地形効果によりほぼ等深線に沿って迂回する傾向がある，などの原因が示唆された。1989年11月に行われた観測では，九州南東で生じた黒潮小蛇行が海山に接近しており，一週間前に行われた観測とは顕著に異なる水温，塩分分布が観測され，短時間の間に大きな海況変化が生じることがわかった。観測地から求めたfL/N(fはコリオリのパラメーター，Lは海山の水平スケール，Nはブラント・バイザラ振動数)で示されるロスビの高さはいずれも駒橋第二海山の頂上推進289 mより低く，また等温線や等塩分線の変化から見積もった傾圧テーラー柱の高さは海面近くまで達しておらず，駒橋第二海山の海底地形効果は上層まで及ばない可能性が示唆された。(*三重大学生物資源学部海洋気候学講座　〒514-8507　三重県津市上浜町1515)

関根義彦* ：九州パラウ海嶺にある駒橋第二海山近辺の海洋構造　第2部　流速場

九州パラウ海嶺中にある海山「駒橋第二海山」の近隣で，1989年から1993にわたり，6回のCTDとADCPによる海洋観測を行った。本論では流速場について報告する。観測されたADCP流速の大半は駒橋第二海山の上を越えて流れており，海山の等深線に層傾向が小さいことが示され，海山の治傾向かがADCP流速の観測深度150-200 mまで達していないことが示唆された。この結果は観測地から見積もったロスビーの高さ(fL/N)が海山の代表深度より小さいこと。等温線や等塩分線の変化から見積もった傾圧テーラー柱が上層まで達していないこと，などの結果と一致する。1989年7月の観測では黒潮小蛇行が発生しており，それに関連して北向きの直線に一致する。1989年7月の観測では黒潮小蛇行が発生しており，それに関連して北向きの直線に一様な強いADCP流速が観測され，一週間の間に大きな海洋変動があることが観測された。ADCP流速の地衡流バランスの達成の割合を地衡流とADCP流速の鉛直速度差を比較することにより調べた。その結果，両者の間には正の相関はあるものの明確な線形の関連は得られず，非地衡流成分が顕著であることが示された。(*三重大学生物資源学部海洋気候学講座　〒514-8507　三重県津市上浜町1515)

La mer 39: 114–119, 2001
Société franco-japonaise d'océanographie, Tokyo

学 会 記 事

1. 2001年3月26日(月)東京水産大学において幹事会(第4回)が開催された。主な議事は下記のとおり。

(1) 報告事項

1．日仏合同シンポジウムの報告があった。
2．平成12年12月11日に日仏関連学会協議会が開催された。
3．クレジットによる海外会員の会費，別刷り代等の支払が可能となった。
4．平成13年度学会賞受賞候補者選考過程が青木委員長から報告された。
5．学会誌 La mer の編集状況が報告された。

(2) 審議事項

1．学会関係の事務，編集作業に関わるコピー代，電話・FAX代は学会が応分の負担を行うこととした。
2．La mer のバックナンバーは申し出があれば，正会員へは安価に提供することとした。
現号(第38巻)まで一括購入の場合は，売価を6万円とすることとした。
3．平成13年度学術研究発表会，総会の日程を5月27日(日)に決定した。
4．研究発表申込期間は4月2日～5月2日とし，本年度より講演要旨集を作成することとした。
5．学会の活性化のために学会賞の見直しを検討することとした。
6．シンポジウム開催の可能性について審議した。
7．日本水産学会より打診のあった，同学会70周年記念大会(10月)において，本学会の概要をパネル展示することについて承認した。また日本海洋学会60周年記念大会(9月)の関連学会合同シンポジウムを協賛することを承認した。

2. 2001年5月14日(月) 東京水産大学において平成13年度幹事会(第1回)および評議員会が開催された。主な議事は下記のとおり。

(1) 報告事項

1．平成14年度科学研究費審査員候補者の推薦を行った

(2) 審議事項

1．平成12年度事業報告
2．平成13年度学会賞受賞候補者選考経過
3．平成12年度収支決算報告および監査報告
4．平成13年度事業計画(案)審議
5．平成13年度収支予算(案)審議
6．その他

3. 新入会員(正会員)

氏名	所属・住所等	紹介者
山口 篤	(株)関西総合環境センター 環境化学部 〒541-0052 大阪市中央区安土町 1-3-5	山口征矢

4. 所属・住所等変更

(正会員・受付順)

加納 敬 〒166-0015 神奈川県藤沢市柄沢 274-1
中村善彦 〒251-0002 神奈川県藤沢市大鋸 3-12-48
谷井潤郎 (財)塩事業センター技術部
〒107-9024 東京都港区赤坂 1-12-32
アーク森ビル24F
千手智晴 九州大学応用力学研究所海洋大気力学部門
〒816-8580 福岡県春日市春日公園 6-1
森谷誠生 〒701-1332 岡山県岡山市平山 747-1
Laurent SEURONT PHD-CNRS
Research Scientist
Station marine de Wimereux
CNRS UPRES-A 8013 ELICO
Universit des Sciences et Technologies de Lille
28 avenue Foch - BP 80, F - 62930 Wimereux, France
内田 裕 海洋科学技術センター海洋観測研究部
〒237-0061 神奈川県横須賀市夏島町 2-15
鷲見浩一 金沢工業大学工学部土木工学科
〒921-8501 石川県石川郡野々市町扇が丘 7-1
岸野元彰 〒338-0832 埼玉県さいたま市西堀 5-2-10-115
内須川正幸 (株)パスコ政策推進部
〒153-0043 東京都目黒区東山 1-1-2
東山ビル4 F

黒田一紀　〒275-0022　千葉県習志野市香澄 1-1-3-406

5. 退会（正会員）

寒川　強，古谷　研，佐々保雄(逝去)，長沼　毅，井上尚文(逝去)

6. 受贈図書(受付順)

国立情報学研究所ニュース　3
NTT R&D　50(4，5)
塩屋崎沖海底地質図説明書　55
なつしま　182，183
農業工学研究所報告　40
東北区水産研究所報告　64
東海大学紀要(一般教養)　26
水産工学研究所研究報告　22
水産光学研究所技報　23
第8回アジア学術会議
日本海区水産研究所研究報告　51
東海大学海洋研究所年報　22
東海大学海洋研究所研究報告　22
Ocean and Polar Research　23(1)
海洋水産研究　21(1-4)，22(1)
ОКЕАНОЛОГИЯ　40(6)
Journal of the Korean Society of Oceanography　36(1)
Annals Hydrographiques　1

日仏海洋学会会則

昭和35年４月７日　制定
昭和60年４月27日　改正
平成４年６月１日　改正

第１条　本会は日仏海洋学会と称する。

第２条　本会の目的は日仏海洋および水産学者の連絡を密にし，両国のこの分野の科学の協力を促進するものとする。

第３条　上記の目的を実現するため本会は次の事業を行なう。

(1)　講演会の開催
(2)　両国の海洋学および水産学に関する著書，論文等の相互の翻訳，出版および普及
(3)　両国の海洋，水産機器の技術の導入および普及
(4)　日仏海洋，水産学者共同の研究およびその成果の論文，映画などによる発表
(5)　両国間の学者の交流促進
(6)　日仏海洋，水産学者の相互の親睦のために集会を開くこと
(7)　会報の発行および出版
(8)　その他本会の目的を達するために必要な事業

第４条　本会には，海洋，水産学の分野に応じて分科会を設けることができる。

分科会は評議員会の決議によって作るものとする。

第５条　本会の事務所は日仏会館（〒150　東京都渋谷区恵比寿３丁目９番25号）に置く。

第６条　本会に地方支部を置くことができる。

第７条　本会会員は本会の目的に賛成し，所定の会費を納めるものとする。

会員は正会員，学生会員および賛助会員とする。

第８条　正会員会費は年額6,000円，学生会員会費は年額4,000円，賛助会員会費は一口年額10,000円とする。

第９条　本会は評議員会によって運営される。

評議員の定数は50名とし，正会員の投票によって選出される。選挙事務は別に定める選出規定による。

会長は評議員会の同意を得て５名までの評議員を追加することができる。

評議員の任期は２年とする。ただし，重任を妨げない。

第10条　評議員はその内より次の役員を選ぶ。ただし，監事は評議員以外からも選ぶことができる。

会長　１名，副会長　２名，幹事　10名，
監事　２名

役員の任期は２年とする。ただし，重任を妨げない。

役員の選出方法は別に定める選出規定による。

第11条　本会に名誉会長，顧問および名誉会員を置くことができる。名誉会長，顧問および名誉会員は評議員会の決議により会長これを委嘱または推薦する。

日仏会館フランス人学長を本会の名誉会長に推薦する。

第12条　会長は本会を代表し，総会および評議員会の議長となる。会長事故あるときは副会長がこれに代わる。

会長，副会長および幹事は幹事会を構成し，本会の庶務，会計，編集，研究発表，渉外などの会務を行う。

監事は本会の会計を監督する。

第13条　年に１回総会を開く。総会では評議員会の報告を開き，会の重要問題を審議する。会員は委任状または通信によって決議に参加することができる。

会長は必要に応じて評議員会の決議を経て臨時総会を招集することができる。

第14条　本会則の変更は総会の決議による。

日仏海洋学会評議員・役員選出規定

1．本規定は日仏海洋学会会則第９条および第10条に基づき本会の評議員および役員の選出方法について規定するものである。

2．評議員は正会員の50名連記無記名投票により選出する。
評議員の選挙事務は庶務幹事が行う。ただし，開票にあたっては本会役員以外の会員２名に立会人を委嘱するものとする。

3．会長は評議員の単記無記名投票により選出する。
会員選挙の事務は庶務幹事が行う。ただし，開票にあたっては本会役員以外の会員２名に立会人を委嘱するものとする。

4．副会長，幹事，および監事は，会長の推薦に基づき評議員会で決定する。

5．本規定の改正は評議員会の議を経て行う。

日仏海洋学会賞規定

1．日仏海洋学会賞（以下「学会賞」という）を本学会に設ける。学会賞は本学会員で，原則として本学会誌に発表した論文の中で，海洋学および水産学において顕著な学術業績を挙げた者の中から，以下に述べる選考を経て選ばれた者に授ける。

2．学会賞受賞候補者を選考するため学会賞受賞候補者推薦委員会（以下「委員会」という）を設ける。

3．委員会の委員は13名とする。
委員は毎年春の評議員会で選出し，委員長は委員の互選により定める。
会長は委員会が必要と認めた場合，評議員会の同意を得て２名まで委員を追加委嘱することができる。

4．委員会は受賞候補１件を選び，12月末までに選定理由をつけて会長に報告する。

5．会長は委員会が推薦した候補者につき無記名投票の形式により評議員会にはかる。投票数は評議員総数の３分の２以上を必要とし，有効投票のうち４分の３以上の賛成がある場合，これを受賞者として決定する。

6．授賞式は翌年春の学会総会において行い，賞状，メダルおよび賞金を贈呈する。賞金は５万円とする。

7．本規定の改正は評議員会の議を経て行う。

覚　書

1．委員は各専門分野から選出されるよう十分配慮すること。

2．受賞者は原則として順次各専門分野にわたるよう十分配慮すること。

日仏海洋学会誌「うみ」投稿規定

1. 「うみ」（日仏海洋学会の機関誌；欧文誌名 **La mer**）は，日仏海洋学会正会員およびそれに準ずる非会員からの投稿（依頼原稿を含む）を，委員会の審査により掲載する。
2. 原稿は海洋学および水産学両分野の原著論文，原著短報，総説，書評，資料などとする。すべての投稿は，本文・原図とも正副2通とする。副本は複写でよい。本文原稿はすべてA4判とし，400字詰め原稿用紙（和文）に，または厚手白紙にダブル・スペース（和文ワープロでは相当間隔）で記入する。表原稿および図説明原稿は，それぞれ本文原稿とは別紙とする。
3. 用語は日，仏，英3か国後の何れかとする。ただし，表および図説明の用語は仏文または英文に限る。原著論文（前項）には約200語の英文または仏文の要旨を，別紙として必ず添える。なお，欧文論文には上記要旨の外に，約500字の和文要旨をも添える。ただし，日本語圏外からの投稿の和文要旨については編集委員会の責任とする。
4. 投稿原稿の体裁形式は最近号掲載記事のそれに従う。著者名は略記しない。記号略号の標記は委員会の基準に従う。引用文献の提示形式は，雑誌論文，単行本分載論文（単行本の一部引用も含む），単行本などの別による基準に従う。
5. 原図は版下用として鮮明で，縮尺（版幅または1／2版幅）に耐えられるものとする。
6. 初校に限り著者の校正を受ける。
7. 正会員に対しては7印刷頁までの掲載を無料とする。ただし，この範囲内であっても色彩印刷を含む場合などには，別に所定の費用を著者負担とすることがある。正会員の投頂で上記限度を越える分および非会員投稿の印刷実費はすべて著者負担（10,000円／頁）とする。
8. すべての投稿原稿について，1篇あたり別刷り50部を無料で請求できる。50部を越える分は請求により50部単位で有料で作製される。別刷り請求用紙は初校と同時に配布される。
9. 原稿の送り先は下記の通り

〒108-8477　港区港南4-5-7　東京水産大学海洋環境学科（山口征矢気付）
日仏海洋学会編集委員会

執　筆　要　領

1. 原稿

(1) 和文原稿の場合：A4判，400字詰横書き原稿用紙に，新かな遣い，常用漢字を用いて楷書体で読みやすく書き，数字は原則としてアラビア数字を使用する。和文ワープロを用いる場合はA4判の用紙におよそ横30字，縦25行で書くこと。

(2) 欧文原稿の場合：A4判の上質の白色用紙に，ダブルスペース約25行にタイプライトし（ワープロの場合も同様），十分な英文添削を経て提出すること。

(3) 和文原稿，欧文原稿いずれの場合も，要旨，表原稿および図版説明原稿はそれぞれ本文原稿とは別紙とする。

(4) 最終原稿とともに，原稿が入力されたフロッピーディスクの提出を歓迎する。この場合ファイルはテキスト形式で保存すること。

2. 論文記載の順序

(1) 原著（和文原稿）：原稿の第1ページ目に表題，著者名と住所（所属機関およびその郵便番号と所在地など）を和文と欧文で記す。またキーワード（4語程度）およびランニングヘッドを添える。第2ページ目に欧文要旨（Abstract，200語以内）を記す，本文は第3ページ目から，「緒言」「方法」「結果」「考察」（あるいは「はじめに」「材料と方法」「結果と考察」など），謝辞，文献，図版の説明の順に記す。なお，原稿には通し番号のページを記入すること。

(2) 原著（欧文原稿）：原稿の第1ページ目に表題，著者名と住所（所属機関およびその郵便番号と所在地など），キーワード（4語程度）およびランニングヘッドを記す。第2ページ目に要旨（Abstract，200語以内）を記す，本文は第3ページ目から，「緒言（Introduction）」「材料と方法（Materials and method）」「結果（Results）」

「考察（Discussion）」「謝辞（Aknowledgement）」「文献（Reference）」「図版の説明（Figure Legends）の順とする。最終ページに，和文の表題，著者名と住所および約500字以内の和文要旨を添える。なお，原稿には通し番号のページを記入すること。

(3) 総説，短報：和文ならびに欧文原稿とも原著に準じる。

(4) 資料，学術情報：特に記載に関する規定はないが，すでに発行されている雑誌を参考にすること。

3. 活字指定

オリジナル原稿の文中で次の活字はそれぞれ朱で指定すること。イタリック指定は下線（＿＿），ボールドあるいはゴシック指定は波下線（〰），スモールキャピタル指定は二重下線（＝＝），中点は・を四角（□）で囲む。上付きおよび下付き文字は∨および∧を入れる。和文原稿での動植物名はカタカナを用い，学名はイタリック指定のこと。なお句読点は（。）および（，）とする。その他の活字指定は編集委員会に一任する。

4. 文　献

文献は本文および図表に引用されたものの全てを記載しなければならない。本文の最後にアルファベット順にまとめ，各文献は下記の例に従って記載する。

(1) 論文の場合

有賀祐勝・前川行幸・横浜康継（1996）：下田湾におけるアラメ群落構造の経年変化．うみ，**34**，45–52.

YANAGI, T., T. TAKAO and A. MORIMOTO (1997): Co-tidal and co-range charts in the South China Sea delived from satellite altimetry data. La mer, **35**, 85–93.

(2) 単行本分載論文（単行本の一部引用）の場合

有賀祐勝（1981）：海洋植物プランクトンの生産生態．藻類の生態（秋山　優・有賀優勝・坂本　充・横浜康継編），内田老鶴圃，東京，p.81–121.

WYNNE, M. J. (1981): Phaeophyta: Morphology and classification. *In* The Biology of Seeweeds. LOBBAN, C. S. and M. J. WYNNE (eds.), Blackwell Science, Oxford, p.52–85.

(3) 単行本の場合

柳　哲雄（1989）：沿岸海洋学―海の中でものはどう動くか―．恒星社厚生閣，東京，154pp.

SVERDRUP, H. U., M. W. JOHNSON and R. H. FLEMING (1942): The Oceans: Their Physics, Chemistry and General Biology. Prentice-Hall, Englewood Cliffs, New York, 1087pp.

5. 図，表および写真

(1) 図，表および写真とその説明はすべて英文または仏文を用いる。

(2) 図は黒インキで明瞭に描き，そのまま印刷できるもののみ受け付ける。図中の線や記号，文字，数字はレンタリング器具などを使用して鮮明に描くこと。原図は原則としてＡ４判以下のサイズにして投稿すること。なおコンピュータのグラフィックソフトを用いて鮮明に描かれた図も受け付ける。この場合プリントアウトはレーザープリンター等を用いて鮮明に打ち出すこと。

(3) 表は別紙にタイプライトすること。

(4) 写真は光沢平滑印画紙（黒白）に鮮明に焼き付け，白地の厚手台紙に貼り付けること。カラー印刷を希望する場合はその旨明記すること。

(5) 図，表，写真は刷り上がり時に最大横が14cm，縦が20cm（説明文を含む）以内であることを考慮して作成すること。

(6) 図，表，写真にはそれぞれ通し番号を付け，１枚ごとに著者名，縮尺ならびに天地を記しておく。図および写真の説明文は別紙にまとめて書き，添付すること。

(7) 図，表，写真の挿入箇所は，本文中に置きたいおよその位置の原稿右欄外に Fig. 1 や Table 1 のように朱書すること。

(8) 地図には方位とスケールを入れること。

6. 単位

時間，濃度，速度，重量，長さ，束（flusx）を表す場合には基本的に SI 単位を用い，本文，図表とも sec, min, hr, d, yr, $\mu g\ l^{-1}$, mg $O_2\ l^{-1}$, cm sec^{-1}, gC $m^{-2}\ d^{-1}$ のような表現を用いること。日付の表示は西暦を用いる。

賛助会員

アレック電子株式会社	神戸市西区井吹台東町７－２－３
株式会社イーエムエス	神戸市中央区多聞通３－２－９
有限会社英和出版印刷	文京区千駄木４－20－６
株式会社内田老鶴圃 内田　悟	文京区大塚３－34－３
財団法人海洋生物環境研究所	千代田区内神田１－18－12　北原ビル
株式会社川合海苔店	大田区大森本町２－31－８
ケー・エンジニアリング株式会社	台東区浅草橋５－14－10
国土環境株式会社	世田谷区玉川３－14－５
三洋測器株式会社	渋谷区恵比須南１－２－８
株式会社高岡屋	台東区上野６－７－22
テラ株式会社	世田谷区代田３－41－８　代田ウエスト５Ｆ
株式会社三菱総合研究所 （社会システム部）	千代田区大手町２－３－６
渡邊機開工業株式会社	愛知県渥美郡田原町神戸大坪230

日仏海洋学会入会申込書

（正会員・学生会員）

	年度より入会	年　月　日申込
氏　名 ローマ時		年　月　日生
住　所　〒 勤務先　機関名 電　話		
自　宅　住　所　〒 電　話		
紹介会員氏名		
送付金額　円	送金方法	
会誌の送り先（希望する方に○をつける）	勤務先　自　宅	

（以下は学会事務局用）

受付	名簿 原簿	会費 原簿	あて名 カード	学会 記事

入会申込書送付先：〒150-0013 東京都渋谷区恵比寿 3-9-25

（財）日仏会館内

日 仏 海 洋 学 会

郵便振替番号：00150−7−96503

2001年5月25日印刷
2001年5月28日発行

うみ　第39巻 第2号

定価 ￥1,600

編集者　山口征矢
発行所　日仏海洋学会
財団法人 日仏会館内
東京都渋谷区恵比寿3-9-25
郵便番号：150-0013
電話：03（5421）7641
振替番号：00150-7-96503
印刷者　佐藤一二
印刷所　㈲英和出版印刷社
東京都文京区千駄木4-20-6
郵便番号：113-0022
電話：03（5685）0621

本雑誌に関する問い合わせ　電話番号 03(5463)0462

うみ

第39巻 第2号

2001年5月

日仏海洋学会